THE CRYSTAL STRUCTURES OF PARA-CHLOR-IODOXY BENZENE AND SOME OTHER AROMATIC COMPOUNDS.

By Elizabeth M. Archer, M.Sc.
(William Porter Scholar of the University of Cape Town).

Thesis presented to the University of Cape Town for the degree of Doctor of Philosophy 1947.

SUMMARY.

The crystal structures of meta-dinitrobenzene, para-chlor-iodoxy benzene, and benzene iodo-dichloride are described.

The structure of meta-dinitrobenzene, ($C_6H_4(NO_2)_2$), was obtained from Fourier projections on the ab and bc planes. The x and y coordinates were obtained with considerable accuracy from the projection on the ab plane, and the z coordinates were obtained from a previous knowledge of the size and shape of the nitro groups and the agreement between the observed and calculated values of F(0kl).

The method of three-dimensional Fourier sections was applied to the crystal para-chlor-iodoxy benzene, ($ClC_6H_4IO_2$), and the coordinates of all the atoms were obtained without any ambiguity. The I-O distances in the iodoxy group are short, which implies the existence of double bonding between the I and O atoms. The main binding forces in the crystal are found to be between neighbouring iodoxy groups.

The structure of benzene iodo-dichloride, ($C_6H_5ICl_2$), has been obtained from Fourier projections on the ac and bc planes. The iodo-dichloride group is linear.

The directions of the covalent bonds of trivalent iodine in $C_6H_5ICl_2$ can be placed in a trigonal bipyramid, but it was impossible to fit the covalent bonds of pentavalent iodine in $ClC_6H_4IO_2$ into any simple geometrical figure.

These iodine compounds were done in order to determine the valency directions of polyvalent iodine, and to see if there was any relationship between the directions of the covalent bonds in trivalent and pentavalent iodine. If such a relationship does exist, it has not yet been detected.

INDEX OF CONTENTS.

THE CRYSTAL STRUCTURE OF

META-DINITROBENZENE.

INTRODUCTION.

Meta-dinitrobenzene forms pale straw-coloured needle-shaped crystals belonging to the orthorhombic system, which melt at 91° C. Von Groth gives the symmetry as orthorhombic bipyramidal, the axial ratios, as determined by Steinmetz (1915) being $\underline{a}$: $\underline{b}$: $\underline{c}$ = 0.9435 : 1 : 0.5434, with the $\underline{c}$ axis in the direction of elongation of the needles. Good, clear crystals may be obtained by slowly cooling a solution in a mixture of alcohol and acetone. Faces giving goniometer reflections develop around the [001] zone, the common ones being (100) and the prism faces (120) and $(1\bar{2}0)$.

The unit cell, as determined by means of X-rays, has the dimensions

$$\underline{a} = 13.3\text{A}$$

$$\underline{b} = 14.1\text{A}$$

$$\underline{c} = 3.80\text{A} ,$$

which correspond to the axial ratios

$$\underline{a} : \underline{b} : \underline{c} = 0.943 : 1 : 0.270 .$$

The indices of the spectra given in this work are referred to these axial ratios and not to those of Steinmetz. Previous attempts to determine the structure of the crystal by means of X-rays have been made by Hertel (1930), Hendricks and Hibbert (1931), and Banerjee and Ganguly (1940). All these workers have assumed the symmetry of the crystal to be orthorhombic bipyramidal, and when the very small value of the $\underline{c}$ spacing is taken into account, this assumption allows only two possible types of structure, both of which are physically improbable and neither of which is consistent with the observed intensities. This was recognised by Hendricks and Hibbert and, shortly after the publication of their paper, it was discovered by Hendricks* that the $\underline{c}$ axis of the crystal was in fact strongly polar when tested for piezoelectricity. This polarity was confirmed by James (unpublished), and has again been tested in the present

* private communication to Professor R.W. James.

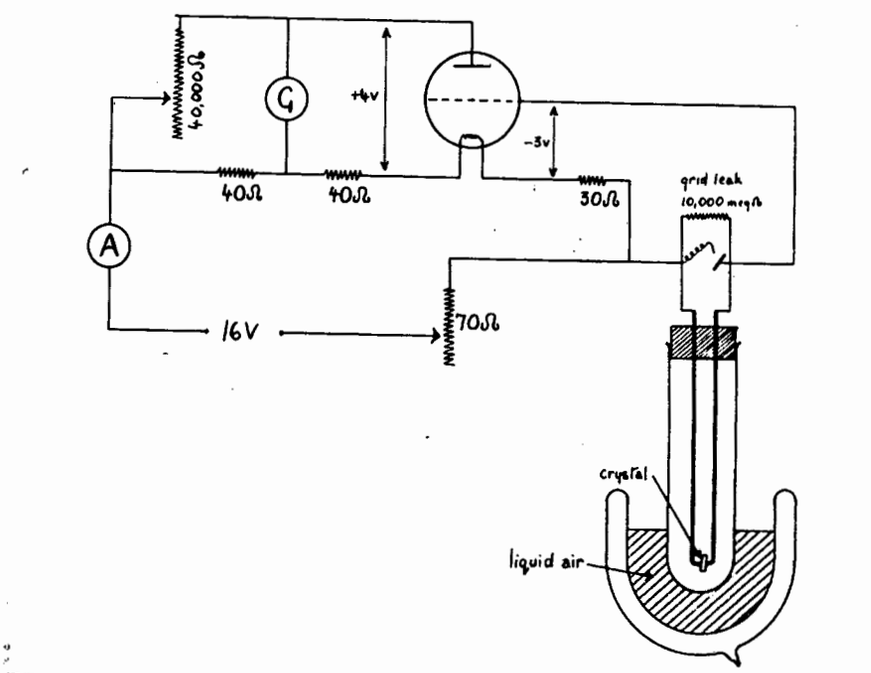

FIGURE I. A diagrammatic representation of the circuit used to measure the polarity of crystals.

THE SPACE GROUP.

The density of the crystal is 1.570 g./c.c., which corresponds to 4 molecules of $C_6H_4(NO_2)_2$ in a unit cell having the dimensions given above.

Oscillation photographs were taken about all three axes with CuK_α radiation. General reflections of all types occur showing that the unit cell is primitive. Reflections 0k$\underline{l}$ occur only with $\underline{k} = 2n$, and h0$\underline{l}$ only with $\underline{h} + \underline{l} = 2n$. There are no restrictions for the hk0 spectra. The possible space groups are Pbn (C_{2v}^9) corresponding to a hemihedral point group, or Pbnm (D_{2h}^{16} or V_h^{16}) corresponding to a holohedral point group. The second of these possibilities is ruled out by the observation that the $\underline{c}$ axis is polar. The space group is therefore Pbn.

PRELIMINARY ESTIMATE OF THE STRUCTURE.

There are 4 molecules in the unit cell, which is the number corresponding to a general position in the space group Pbn. Nothing in the structure is therefore fixed by symmetry. Had the space group been Pbnm, the assumption made by previous workers, the general positions would have been eightfold. In order to reduce the number of molecules in the unit cell to 4, it would therefore have been necessary to suppose the mirror planes possessed by this group to be also planes of symmetry of the molecule. The small $\underline{c}$ spacing, 3.8Å, which is about the known thickness of the benzene ring, would make it necessary to suppose the benzene rings themselves to lie on mirror planes. The nitro groups would then have to lie either with all their atoms on the mirror planes also, or with the nitrogen atoms on the mirror planes and the oxygen atoms symmetrically disposed on either side of them. The first of these possibilities is negatived at once by the observed intensities, for it would give a very strong 002 spectrum, whereas 002 is, in fact, very weak.

The second type of arrangement would reduce the intensity of the 002 spectrum but would bring the oxygen atoms in adjacent molecules improbably close to one another, The distance obtained by Hendricks and Hibbert is 1.91Å, whereas distances of over 3Å have been found in other aromatic compounds, and distances of 2.7A in inorganic compounds. The structure proposed by Banerjee and Ganguly is also of the same type and is subject to the same objections as that of Hendricks and Hibbert. The latter workers were alive to these difficulties, and, because of them, Hendricks suggested that the crystal was polar, as has already been stated in the introduction.

If the space group is assumed to be Pbn, it is no longer necessary to suppose the benzene rings to lie on mirror planes. Nevertheless, there is a good deal of evidence for the view that the planes are not greatly inclined to the plane (001).

The three principal refractive indices of the crystal, determined by James and Horrocks, are, for sodium light,

$$\alpha = 1.48$$

$$\beta = 1.68$$

$$\gamma = 1.71 ,$$

corresponding to vibrations parallel to c, b, and a respectively as shown in fig. 2 . The small refractive index for vibrations parallel to c indicates that the c axis is nearly perpendicular to the planes of the benzene rings, while the relative magnitude of β and γ indicate that the planes of the rings are nearly parallel to a and inclined at a not very large angle to b.

An examination of the diffuse reflections, the optical ghosts due to thermal vibrations, accompanying some of the spectra, points in the same direction. Laue photographs taken with unfiltered copper radiation when the c axis is vertical show a remarkable set of diffuse reflections in positions corresponding to the first layer lines of a rotation photograph about the same axis. A reproduction of such a Laue photograph taken on a cylindrical camera is shown in fig. 3 . The ghosts

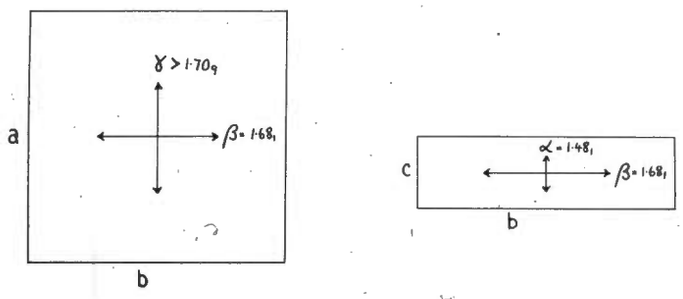

FIGURE 2. The principal refractive indices of the crystal meta-dinitrobenzene.

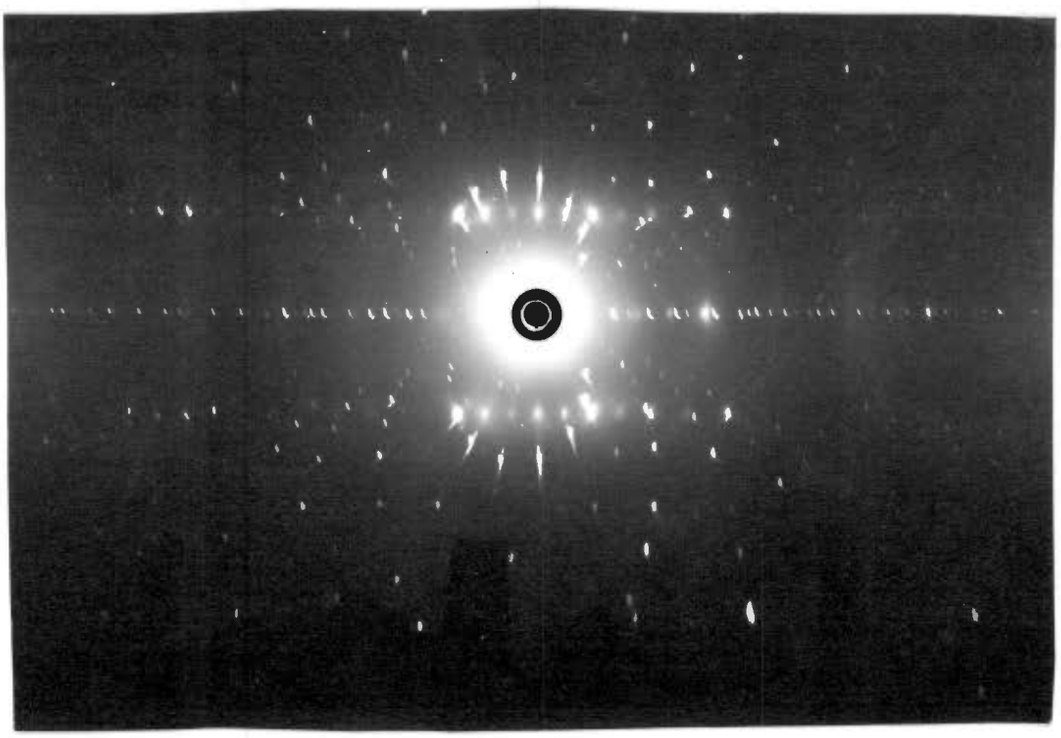

FIGURE 3. A Laue photograph of meta-dinitrobenzene, taken on cylindrical film, and showing clearly the "layer-lines" of ghosts, superimposed on the ellipses of the Bragg spots.

accompanying the spectra 021 and $0\bar{2}1$ are particularly strong and diffuse and are of the layer lattice type. (Lonsdale, 1942) This suggests that the planes of the benzene rings lie not far from the (021) and ($0\bar{2}1$) planes.

In making use of these data to estimate a preliminary structure of the crystal it was assumed that the benzene ring was a regular hexagon of side 1.4Å, and the size and shape assumed for the nitro groups were based on the results of James, King and Horrocks (1935) for para-dinitrobenzene and of van Niekerk (1943) for 4:4'-dinitrodiphenyl. Three dimensional cardboard models were constructed to scale and packed into the unit cell in such a way as to fulfil the symmetry conditions, and to conform to the arrangements suggested by the refractive indices and the thermal ghosts. It was found that there were a large number of ways in which these molecules could pack into the unit cell.

RELATIVE INTENSITY MEASUREMENTS.

All the observations were photographic, and were made with a cylindrical camera with CuK_α radiation filtered through nickel foil. Neither an ionization spectrometer nor an integrating photometer was available, so that it was not possible to obtain absolute measurements of intensity and a set of relative measurements had to suffice.

A crystal of 0.25mm. uniform cross-section was mounted for rotation about the c axis and the intensities of the spectra hk0 on the zero layer line were measured.

The film was passed in front of a photographically recording microphotometer. A typical photometer trace of the zero layer line of one of the films is shown in fig. 4 .

The variation in intensity with the height of the peak

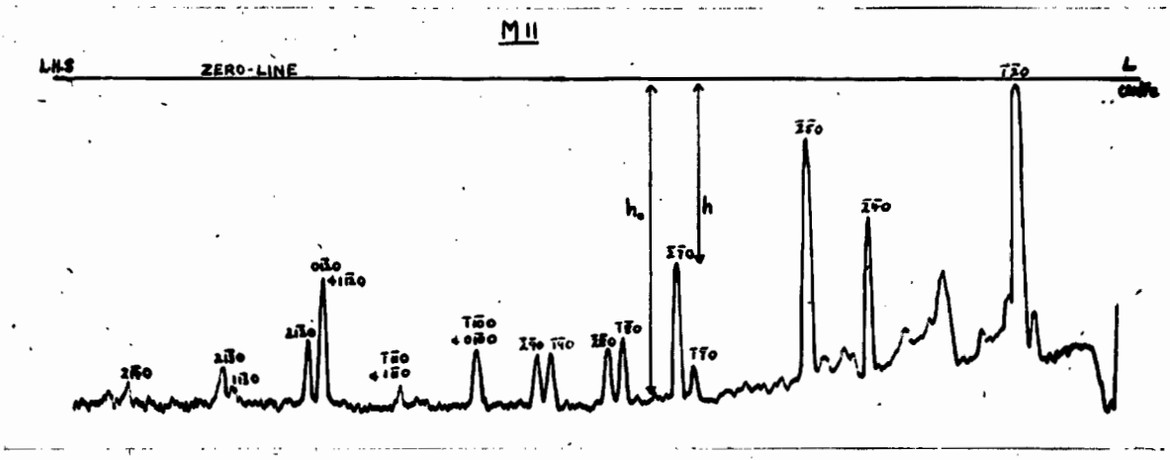

FIGURE 4. A reproduction of the microphotometer trace of the zero layer line (left-hand side) of the film M11.

TABLE 1. THE RELATIVE INTENSITIES OF THE SPECTRA APPEARING ON THE LEFT-HAND SIDE OF FILM M 11.

Spectrum	h_o	h	I_o	I	I-I_o
$\bar{1}20$	6.8	0.15	1	>220	v.s.
$\bar{2}40$	7.7	3.6	-3	25	28
$\bar{2}50$	7.7	1.55	-3	59	62
$\bar{1}70$	8.3	7.45	-6	-2	4
$\bar{2}70$	8.3	4.8	-6	14	20
$\bar{1}80$	8.4	6.75	-7	2	9
$\bar{2}80$	8.4	7.05	-7	0	7
$\bar{1}90$	8.55	7.15	-7	0	7
$\bar{2}90$	8.5	7.15	-7	0	7
$\bar{1},\bar{10},0$ & $0,\bar{10},0$	8.5	7.05	-7	0	7
$1,\bar{11},0$ & $1,\bar{11},0$	8.5	8.0	-7	-5	2
$0,\bar{12},0$ & $1,\bar{12},0$	8.45	5.2	-7	11	18
$2,\bar{12},0$	8.4	6.8	-7	1	8
$1,\bar{13},0$	8.45	8.05	-7	-5	2
$2,\bar{13},0$	8.4	7.6	-7	-3	4
$2,\bar{14},0$	8.5	7.95	-7	-5	2

TABLE 2. THE STANDARDISATION OF THE LEFT HAND SIDE OF FILM M11 WITH THE LEFT HAND SIDE OF FILM M 12.

Spectrum	I - I_o		Ratio $\frac{\text{M 11}}{\text{M 12}}$.
	M 11	M 12	
$\bar{2}40$	28	23	1.2
$\bar{2}50$	62	62	1.0
$\bar{2}70$	20	19	1.05
$\bar{2}80$	7	7	1.0
$\bar{2}90$	7	7	1.0
$0,\bar{12},0$ & $1,\bar{12},0$	18	13	1.4
$2,\bar{12},0$	8	6	1.3

mean ratio = 1.1

was determined by Dr. J.N. van Niekerk of the University Physics Department. He made a series of standard wedges of known exposure from the direct X-ray beam, which were then photometered and the relationship between h (The distance in cms. from the zero-line to the trace) and I (the intensity in seconds of exposure time) obtained. A graph of I against h was drawn using these values and from this intensity curve the relative intensities of the spectra, appearing on the photometer curves for the film, were determined as follows:

Values of h and h_o were measured, where h is the distance from the zero-line to the top of the peak and h_o is the distance from the zero-line to the background on which the peak occurs. The corresponding values of I_o and I were found from the intensity curve and the relative intensity of the spectrum is $(I - I_o)$. The relative intensities of the spectra appearing on the trace shown in fig. 4, are given in Table 1.

Since no Weissenberg camera was available at this stage many oscillation photographs were necessary in order to get the full rotation of the crystal required (90°) and, although care was taken to expose and develop the films for the same length of time, it was impossible to record each film under exactly the same conditions. For each film, therefore, oscillations of 15° were given to the crystal, which was then turned through 10° for successive films until the full rotation had been obtained. In this way successive films had common spectra which were used to standardize the films in terms of one another. The standardisation of two successive films in this way is shown in Table 2. Thus the intensities of the spectra on all the films were expressed on the same scale.

When making these intensity observations it was found that several low order spectra were overexposed. Any peaks with $h < 0.3$ cms. were assumed to be overexposed. It was therefore necessary to take further films with reduced exposure times to

include these strong spectra as well as other spectra of determined intensity, by comparison with which the strong spectra could be expressed on the same scale. The assumption was made that the heights of the peaks on the photometer trace, properly calibrated, were proportional to the integrated reflections of the corresponding spectra. This procedure, although it has little theoretical justification, is found empirically to lead to no inconsistencies, and is certainly a much better approximation to the truth than can be obtained by mere visual estimation. The intensities so measured, are, of course, on an arbitrary scale. They can then be multiplied by a suitable factor in order to give approximately absolute intensity values.

When an arrangement was found that gave the same general rise and fall of intensities as those observed it was possible to express the observed intensities on an approximately absolute scale for the purpose of carrying out the Fourier synthesis. It may here be pointed out that if the wrong absolute scale has been chosen the only effect on the Fourier projection will be to make the relation of the peaks to the background wrong. The projection would be useless for an electron count. On the other hand, the positions of the peaks will not be appreciably affected and these are all that are required for a structure determination. If the relation between weak and strong integrated reflections is wrongly given, this may have some effect on the positions of the peaks in the projection, but it will not be a large effect unless the error is very considerable. A systematic error with increasing order of spectrum will have the effect of a false temperature effect and will alter the sharpness of the peaks, but not appreciably the positions of their maxima.

STRUCTURE FACTOR CALCULATIONS.

The coordinates of a point in a general position for the space group Pbn are

$$(x,y,z)\ ,\ \left(\tfrac{1}{2}-x,\ \tfrac{1}{2}+y,\ z\right)\ ,\ \left(\tfrac{1}{2}+x,\ \tfrac{1}{2}-y,\ \tfrac{1}{2}+z\right),\ \left(\bar{x},\bar{y},\ z+\tfrac{1}{2}\right).$$

The general structure factor F(hkl) is given by

$$F(hkl) = \sum_s f_s \left(A_s + i B_s\right)$$

The structure factors used in this work are F(hk0) and F(0kl):

For F(hk0) when $h+k = 2n$, $\begin{cases} A = 4\cos 2\pi hx \cos 2\pi ky \\ B = 0 \end{cases}$

when $h+k = 2n+1$, $\begin{cases} A = -4\sin 2\pi hx \sin 2\pi ky \\ B = 0 \end{cases}$

For F(0kl) when $k = 2n$ and $l = 2n$, $\begin{cases} A = 4\cos 2\pi ky \cos 2\pi lz \\ B = 4\cos 2\pi ky \sin 2\pi lz. \end{cases}$

when $k = 2n+1$ and $l = 2n+1$, $\begin{cases} A = -4\sin 2\pi ky \sin 2\pi lz \\ B = 4\sin 2\pi ky \cos 2\pi lz \end{cases}$

f_s is the atomic scattering factor of the atom s in the unit cell, whose coordinates are (x_s, y_s, z_s), and the summation is to be taken over all the atoms in the unit cell. For carbon, the atomic scattering factors given by Robertson (1935), which were derived from measurements on anthracene at low temperatures, were used. For nitrogen and oxygen the values tabulated by James and Brindley (1931) were used as basis, but they were reduced in the same ratio as that between Robertson's values for carbon and those of James and Brindley, in order to make some allowance for thermal motion.

The provisional structure was adjusted until the observed structure factors of the strongest spectra of type hk0 agreed with those calculated from the above formulae using the assumed coordinates. In calculating the observed structure factors it

was assumed that the crystals reflected as mosaics, so that the intensities were proportional to the squares of the structure factors. It was found possible to get fair agreement with two types of packing, and these were tested by means of a Fourier projection.

THE FOURIER SYNTHESIS.

The projection of the structure on the plane (001), which uses spectra of the type hk0, is the most suitable for the purpose. The density $\sigma(x,y)$ of the projection at the point (x,y) on the plane ab is given by

$$\sigma(x,y) = \frac{1}{A(ab)} \sum_{h=-\infty}^{+\infty} \sum_{k} F(hk0) \exp\left[-2\pi i\left(\frac{hx}{a} + \frac{ky}{b}\right)\right],$$

where A(ab) is the area of the side ab of the unit cell. The projection has a centre of symmetry, although the structure as a whole has not, and the series in this case takes the form

$$\sigma(x,y) = \frac{1}{A(ab)} \sum_{h=-\infty}^{+\infty} \sum_{k} \pm |F(hk0)| \cos 2\pi\left(\frac{hx}{a} + \frac{ky}{b}\right)$$

The observed values of $|F(hk0)|$ are used as the coefficients in the series, the sign appropriate to any given coefficient being determined from the provisional structure. The two types of packing that gave possible magnitudes to the calculated structure factors for the strong spectra gave opposite signs to some of them and the Fourier projection was made with each set of signs in turn, the method used being substantially that described by Lipson and Beevers (1936). One set of signs gave a projection corresponding to nothing physical, but the other gave very clear outlines of the molecules. From this projection, more accurate values of the x and y parameters were determined a recalculation of the structure factors was made, which resulted in a change of sign of some of the smaller coefficients, and a

TABLE 3. COMPARISON OF OBSERVED AND CALCULATED F VALUES.

Spectrum	4 F_{obs}	F_{calc}	Spectrum	F_{obs}	F_{calc}
200	23.6	-19.2	240	12.4	-12.8
400	34.0	46.8	250	22.0	-21.6
600	50.8	42.8	260	abs.	- 6.4
800	abs.	0	270	15.2	-16.4
10,00	10.0	12.4	280	9.6	8.0
12,00	abs.	8.4	290	10.8	- 9.6
			2,10,0	abs.	- 4.4
020	27.6	32.0	2,12,0	12.8	10.8
040	27.3	-32.0	2,13,0	9.6	14.4
060	33.2	-42.0			
080	17.0	-16.0	310	53.2	-59.6
0,10,0	5.6	4.8	320	abs.	6.8
0,12,0	18.6	-22.8	330	25.2	22.0
			340	12.8	-13.6
110	10.8	-13.6	350	14.0	13.6
120	25.6	18.8	360	43.2	-51.6
130	43.6	53.2	370	17.6	19.6
140	34.4	-45.2	380	abs.	- 2.4
150	10.8	- 5.2	390	7.3	-13.2
160	16.8	13.6	3,10,0	abs.	7.2
170	6.4	- 5.4			
180	10.4	10.8	410	5.6	- 1.2
190	10.0	-17.2	420	21.2	-22.0
1,10,0	10.0	19.2	430	10.0	- 5.6
1,11,0	10.8	5.2	440	abs.	2.0
1,13,0	6.4	- 7.2	450	15.2	16.8
			460	8.4	-14.8
210	26.0	-30.0	470	abs.	- 2.8
220	23.2	-30.4	480	6.8	1.2
230	31.2	-37.6	490	8.0	- 3.6

TABLE 3 . (continued)

Spectrum	4 F_{obs}	F_{calc}	Spectrum	4 F_{obs}	F_{calc}
4,10,0	10.8	19.6	810	abs.	1.6
			820	10.0	- 8.8
510	14.8	-12.8	830	9.2	14.4
520	33.6	-34.4	840	12.8	-15.2
530	13.2	10.0	850	abs.	4.0
540	12.4	-20.4	860	14.8	- 9.3
550	abs.	- 2.0	870	16.4	-22.4
560	16.4	16.8	880	14.8	16.8
570	16.4	25.2	890	16.0	-18.8
580	15.2	22.4			
590	abs.	- 4.8	910	abs.	3.2
			920	abs.	5.2
610	abs.	- 7.3	930	5.2	7.2
620	14.0	-16.0	940	4.8	6.0
630	3.9	- 1.2	950	abs.	- 2.4
640	abs.	5.2	960	15.6	-10.4
650	abs.	5.2	970	abs.	8.8
660	abs.	- 0.8	980	10.0	13.6
670	5.2	5.2			
680	abs.	1.2	10,10	abs.	- 2.4
6,12,0	6.8	-11.6	10,20	abs.	- 8.8
			10,30	10.0	11.6
710	34.0	-36.8	10,40	12.4	20.4
720	16.0	23.2	10,50	22.4	25.2
730	8.0	5.2	10,60	abs.	- 4.0
740	8.8	- 8.0	10,70	12.0	13.6
750	abs.	5.2	10,80	13.2	-14.8
760	abs.	- 2.4			
770	9.2	16.0	11,60	9.6	11.6
780	abs.	- 2.8	11,70	6.8	8.0

TABLE 3. (continued)

Spectrum	4 F_{obs}	F_{calc}	
11,80	8.4	3.2	
12,60	6.8	-11.6	
13,10	7.2	10.8	
13,20	4.8	-10.8	
			δ
021	60	67.6	278°
041	25	17.3	35°
061	25	34.8	290°
081	10	11.7	198°
0,10,1	12	19.5	259°
0,12,1	abs	10.2	62°
002	6	6.6	76°
022	38	18.8	177°
042	26	7.1	344°
062	8	15.7	289°
082	12	18.0	288°
0,10,2	15	9.9	76°
023	abs	9.6	222°
023	abs	9.6	222°
043	8	11.6	196°
063	13	16.2	98°
083	9	14.1	98°

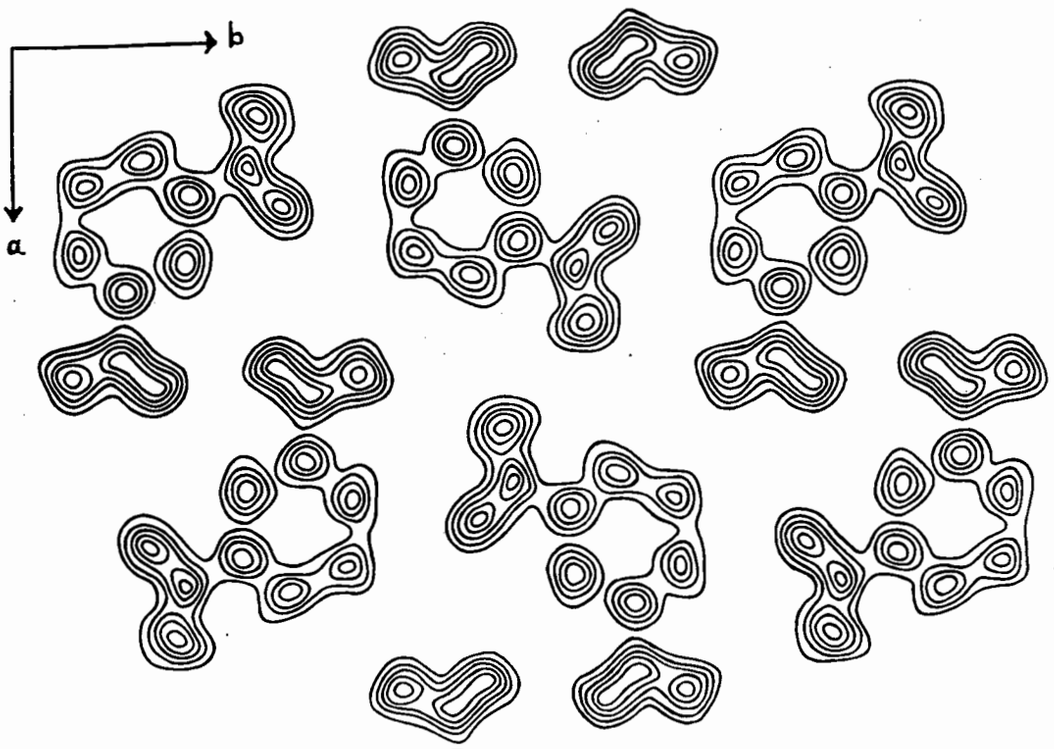

FIGURE 5. Fourier projection of the structure in the c direction on the ab plane. Contours are drawn at intervals of approximately 1 electron per sq.A. The outer line is the 2-electron contour.

second projection was carried out. A third and final projection was made as a result of the second, and this is illustrated in fig. 5, which may be considered in conjunction with the key diagram fig. 6.

The agreement between F (observed) and F (calculated) (for the third projection) is good, with no serious discrepancies. Table 3 shows the agreement between the observed and calculated F values for the spectra hk0 and 0kl.

ESTIMATION OF PARAMETERS.

In the projection on the c face the atoms are all well resolved, and it is possible to fix the x and y parameters with considerable accuracy. From these, in conjunction with the known dimensions of the molecule, it is possible to draw certain conclusions. The lines joining opposite carbon atoms of the benzene ring pass very nearly through one point in the middle of the ring. This suggests that the hexagon is regular, but the different lengths of the sides indicate that the plane of the ring is not parallel to the (001) plane. The lengths of the sides nearly parallel to the a axis are 1.41A, but the other sides have in the projection a length 1.33A. If the ring is regular, it must make an angle of about 20° with the b axis and be nearly parallel to the a axis. This result is in agreement with the results of Banerjee and Bhattacharjya, of which it has been possible to obtain only an abstract, who from measurements of the magnetic anisotropy of the crystals conclude that the benzene ring is parallel to the a axis , but is inclined at an angle of 22° 20′ to the b axis. In the projection the C_1-N_1 distance is 1.40A, the C_3-N_2 distance is 1.33A. Allowing for the above-mentioned tilt of the molecule of 20° to the b axis, the CN distances become 1.42A, if it is assumed that the CN link lies

in the plane of the benzene ring. These CN distances are shorter than the CN distances observed by James et al. (1935) for para-dinitrobenzene and van Niekerk (1943) for 4:4'-dinitrodiphenyl the average value of which is 1.54A. The discrepancy can be explained by assuming the CN link to be inclined at an angle of about 15° to the plane of the ring. In fig. 6, if the directions of the arrows on the molecules indicate a tilt downwards, then N_2 is below the plane of the ring and N_1 could either be above or below C_1.

TABLE 4. INTERATOMIC DISTANCES IN THE NITRO GROUP (IN A).

	C-N	N-O_1	N-O_2	O-O
para-dinitrobenzene	1.53	1.25	1.10	2.14
4:4'-dinitrodiphenyl	1.56	1.21	1.14	2.00
complex of 4:4'-dinitrodiphenyl with 4-hydroxydiphenyl	1.53	1.10	1.10	1.90

The N-O distances in the projection are all different, and this suggests that the nitro groups do not lie in the (001) plane. James et al. (1935) and van Niekerk (1943) found the nitro group to be unsymmetrical, and the values of the interatomic distances obtained by them are given in Table 4. In neither case were the observations accurate enough to make this lack of symmetry entirely certain. A symmetrical nitro group has been observed in some recent work by Saunder (1946), on a molecular complex of 4:4'-dinitrodiphenyl and 4-hydroxydiphenyl, in which the nitro groups are found to lie across a mirror plane of symmetry. Various possible N-O distances were assumed, and the corresponding z parameters calculated for both possible positions of each oxygen atom in relation to the corresponding nitrogen atom, and for both possible positions of N_1 relative to C_1. These z parameters were checked by comparing the calculated and observed

F values for the 0kl spectra. The best agreement was obtained with the nitro group symmetrical, the N-O distance being 1.20A, as shown in fig. 9 . It was found that the angle $\hat{ONO}$ was then 130° and the O-O distance 2.17A. These values are in agreement with those obtained by James et al. (1935), van Niekerk (1943), and Saunder (1946).

An examination of fig. 8 , which shows the positions of the atoms in the crystal projected on to the bc plane, shows that the overlap of the molecules is such that no very good resolution is to be expected, particularly as the number of spectra available for the projection is small, owing to the small value of the c spacing and to space group restrictions. Similar remarks apply to the projection on the ac plane. However, a projection of the electron density on the bc plane was made, using visual estimates of the intensities of the spectra F(0kl) . In this projection there is no centre of symmetry, so it was necessary to calculate the phases in order to carry out the summation. This projection is shown in fig. 7 . No definite values for the parameters could be obtained from this projection, but the large unresolved peaks are quite consistent with the arrangement of atoms shown in fig. 8 . It is worth noting that the molecules lie very nearly in the planes (021) and $(0\bar{2}1)$, which would account for the strong thermal ghosts of the layer lattice type that accompanies the corresponding spectra.

The parameters of the atoms, expressed as fractions of the lattice translations, are shown in Table 5.

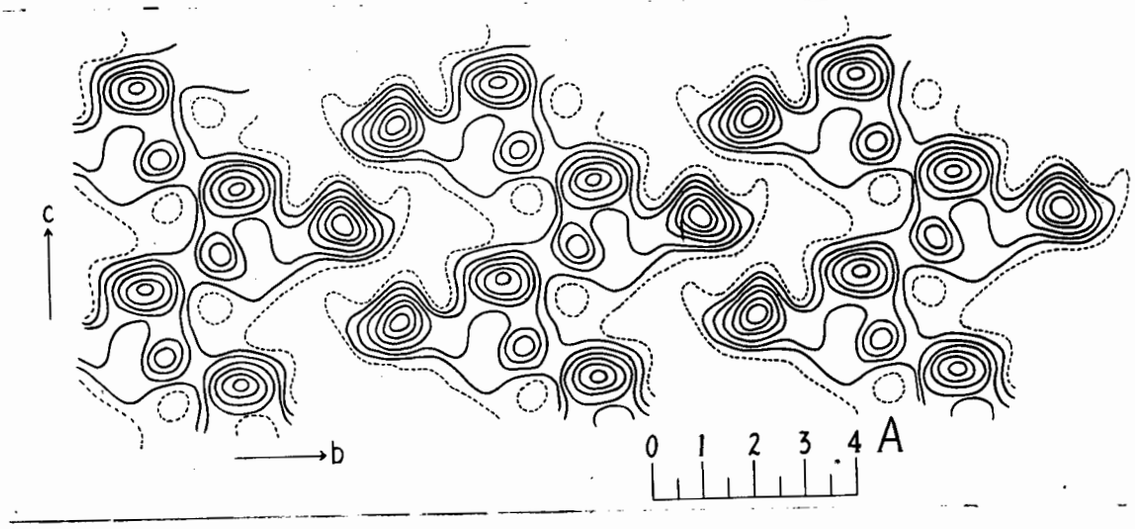

FIGURE 7. Fourier projection of the structure in the a direction onto the bc plane. The contours are drawn at equal intervals.

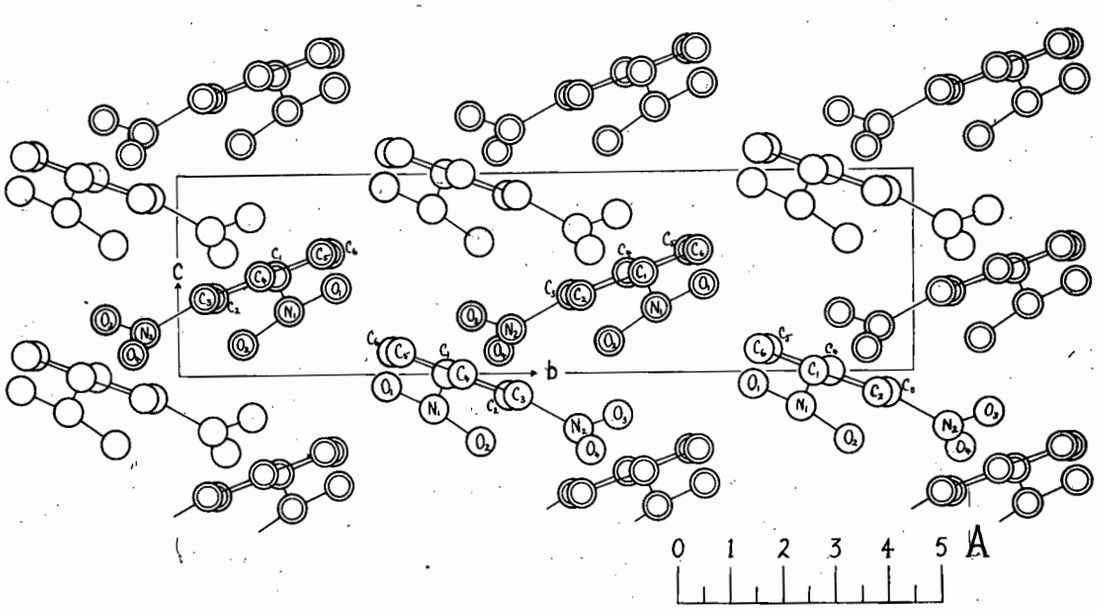

FIGURE 8. Projection of the structure in the a direction onto the bc plane. The molecules with double circles are a/2 above or below those with single circles.

TABLE 5. PARAMETERS OF THE ATOMS EXPRESSED AS FRACTIONS OF THE CORRESPONDING LATTICE TRANSLATIONS.

	x	y	z
C_1	0.135	0.367	0
C_2	0.180	0.452	-0.109
C_3	0.285	0.463	-0.109
C_4	0.347	0.388	0
C_5	0.300	0.304	0.109
C_6	0.197	0.292	0.109
N_1	0.082	0.354	-0.174
N_2	0.333	0.546	-0.283
O_1	-0.003	0.284	+0.063
O_2	-0.017	0.411	-0.345
O_3	0.268	0.601	-0.213
O_4	0.416	0.564	-0.388

DESCRIPTION OF THE MOLECULE.

From the calculations already described, the molecule has the following dimensions:

C-C = 1.41A, C-N = 1.54Å, N-O = 1.20A, O-O = 2.17A.

The size and shape of the molecule is given in fig. 9 .

It must be understood that this picture of the molecule of meta-dinitrobenzene has been derived from only one projection (that on the ab plane), and the size and shape of the nitro group has been largely assumed from the results obtained for other nitro compounds. This description refers to the molecule as a unit of the crystal structure, and a free molecule may not necessarily have the same configuration.

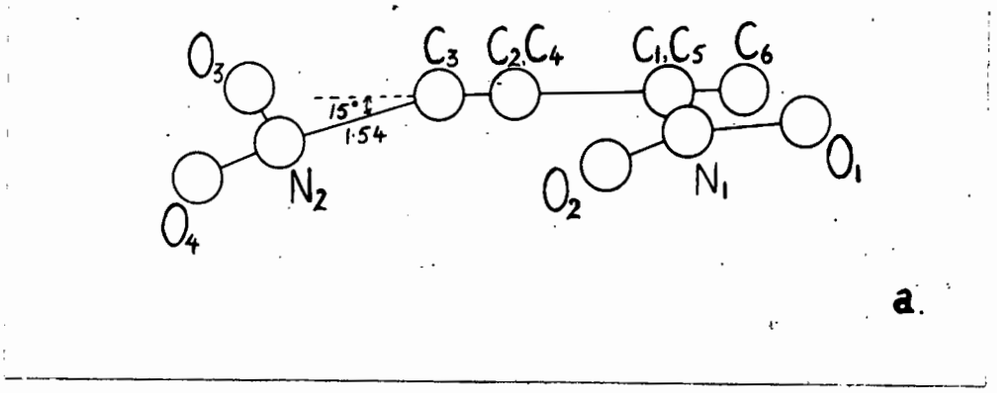

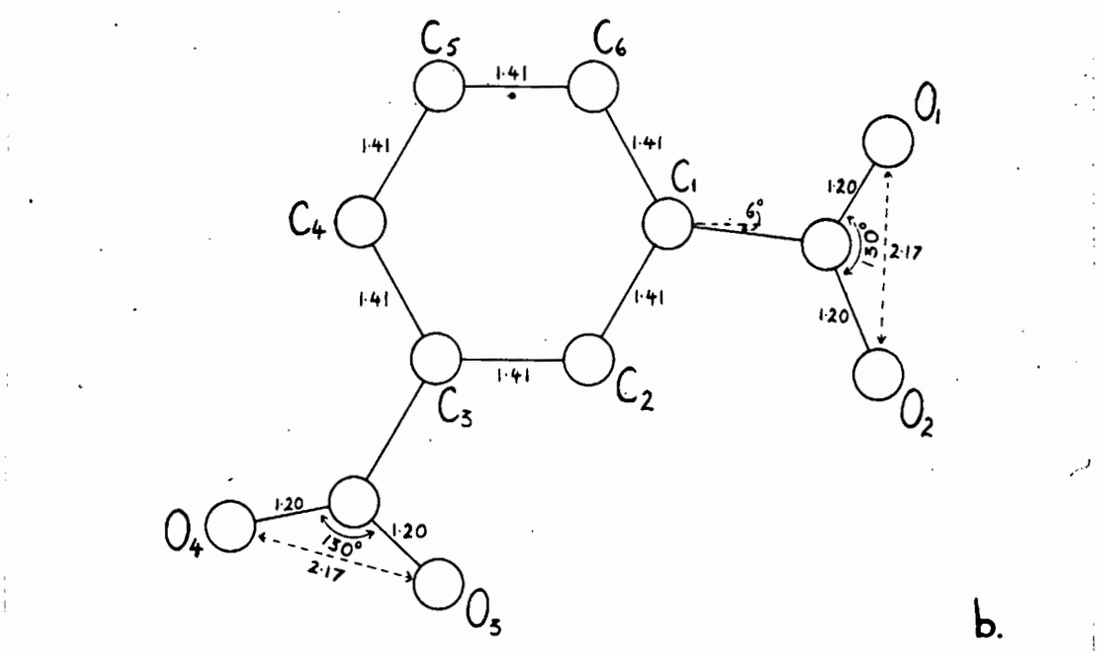

FIGURE 9. a. The molecule of meta-dinitrobenzene projected on to a plane normal to that of the benzene ring.

b. The molecule of meta-dinitrobenzene projected on to the plane of the benzene ring.

Note: In fig. 9b, the angle of 6° which the projected line joining $C_1 N_1$ makes with the line $C_1 C_4$ may be due to N_1 and O_2 being unresolved in the projection (see fig.5) and may not be a real effect.

THE PACKING OF THE MOLECULES IN THE CRYSTAL.

There are 4 molecules in the unit cell which are derived from a single molecule by operation of the glide planes. The diagrams are labelled so that atoms derived from one another by a lattice translation, or by the operation of a glide plane are denoted by the same letter.

The packing of the molecules in the crystal is such that each oxygen atom approaches one CH unit rather closely (the distances of approach varying from 2.95A to 3.25A) and the other CH units at a much greater distance (these distances varying from 3.55A upwards). There seems to be no tendency for an oxygen atom to pack itself at equal distances from neighbouring CH units. These shortest distances can be compared with the O-CH distance of 3.3—3.4A obtained by James et al. (1935) with para-dinitrobenzene and the O-CH distances of 2.9—3.2A and 3.4—3.6A obtained by van Niekerk (1943) with 4:4'-dinitrodiphenyl.

The closest approach of CH units to one another is 3.6A, which is in agreement with other work done on aromatic compounds.

The closest approach of neighbouring oxygen atoms varies from 3.2A to 3.7A, which distance is considerably greater than the closest distance of approach for O-O in inorganic compounds, which is 2.7A, but agrees with the values obtained by James et al. and van Niekerk for aromatic nitro compounds.

The forces binding the crystal together are probably van der Waals' forces, although it seems possible that there may be some attractive force between neighbouring O and CH units which helps to bind the crystal together.

The structure is a compact one. The crystal has a high density, 1.57 g./c.c., and, like other organic crystals, is fairly soft and easily cut. It is unlike para-dinitrobenzene and 4:4'-dinitrodiphenyl in this respect, although the main binding forces of the crystal appear to be of the same type.

NOTE.

Almost simultaneously[14] with the publication of the above crystal structure of meta-dinitrobenzene in the Proceedings of the Royal Society (Dec. 1946), a paper "The Crystal Structure of Meta-dinitrobenzene" by N.W. Gregory and E.N. Lassettre was published in the Journal of the American Chemical Society (Jan. 1947). This structure is essentially the same as the one already described. The space group is Pbn, and a Fourier projection on the ab plane was made, using the spectra of type hk0. The x and y coordinates are the same within the limits of experimental error. Their z coordinates, however, are very different from those quoted above. Gregory and Lassettre calculated their z coordinates from an examination of the hkl spectra appearing on the 1st layer line of rotation photographs taken with the crystal rotating about the c axis. They assumed that the nitro groups were in the same plane as the benzene ring.

The dimensions of the molecule of meta-dinitrobenzene are given in the following table which appeared in their paper.

"Inter-atomic Distances in A.

$C_1 - C_2 = 1.33$	$N_1 - O_1 = 1.18^*$
$C_2 - C_3 = 1.33$	$N_1 - O_2 = 1.10^*$
$C_3 - C_4 = 1.42$	$N_2 - O_3 = 1.15$
$C_4 - C_5 = 1.38$	$N_2 - O_4 = 1.22$
$C_5 - C_6 = 1.37$	$O_1 - O_2 = 1.95^*$
$C_6 - C_1 = 1.37$	$O_3 - O_4 = 2.13$
mean = 1.37	$O_3 \hat{N}_2 O_4 = 128°$
$C_2 - N_1 = 1.46^*$	$O_1 \hat{N}_1 O_2 = 120°^*$
$C_6 - N_2 = 1.39$	

* indicating less reliable distances "

Gregory and Lassettre then state, "The average carbon-carbon distance agrees within experimental error with the accepted

value of the carbon-carbon distance in the benzene ring. The carbon-nitrogen distance in m-dinitrobenzene is 1.39 ± .04Å. This inter-atomic distance corresponds to 18% double bond character for the carbon-nitrogen bond". The possibility that the carbon-nitrogen link might not lie in parallel to the ab plane was not considered as an explanation of the shortness of this distance compared with the C-N distances obtained by James et al. (1935) and van Niekerk (1943) on aromatic nitro compounds.

Gregory and Lassettre consider the attraction between atoms of different molecules to be of two types; first, those between oxygen and hydrogen atoms and, second, those between benzene nuclei. They suggest that hydrogen bonds are formed in the cases where the distance from O to CH unit is small, namely 3.0Å, and further state that the association of m-dinitrobenzene in benzene solution is to be attributed in part to this fact.

THE CRYSTAL STRUCTURE OF

PARA-CHLOR-IODOXY BENZENE.

PREPARATION AND DESCRIPTION OF THE CRYSTALS.

The para-chlor-iodoxy benzene and the para-methyl-iodoxy benzene used in the experiments was prepared by Dr. W.S. Rapson of the University Chemistry Department.

Para-chlor-iodoxy benzene gradually separated when a solution of para-chlor-iodo benzene in ether was shaken with an excess of Caro's acid for several days. (c.f. Bamberger and Hill (1900)). It was filtered off from the reaction mixture, and well washed with water. Pure crystals, having the same properties as the material described by Willgerodt (1893), were subsequently grown from this product. Para-methyl-iodoxy benzene was prepared in a similar way.

Fairly good crystals of both compounds were grown from water and also from glacial acetic acid. They have the form of colourless, thin flat plates with the a faces predominant and a cleavage plane (001).

The shapes of the crystals are shown in the following sketch.

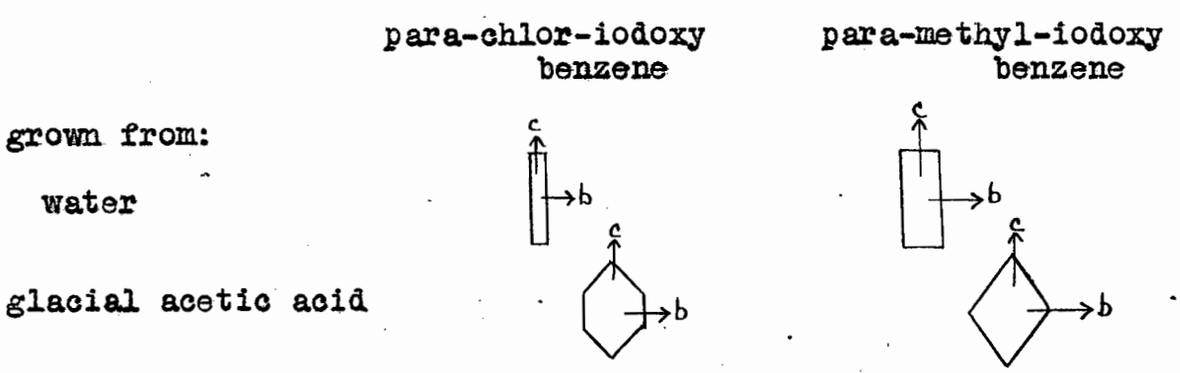

Photographs were taken with all the crystals, and it was found that the crystal para-methyl-iodoxy benzene is identical with the crystal para-chlor-iodoxy benzene with regard to its unit cell, space group, and intensities of spectra. A complete structural determination was then made of para-chlor-iodoxy benzene using crystals grown from acetic acid, as these were slightly thicker than those grown from water.

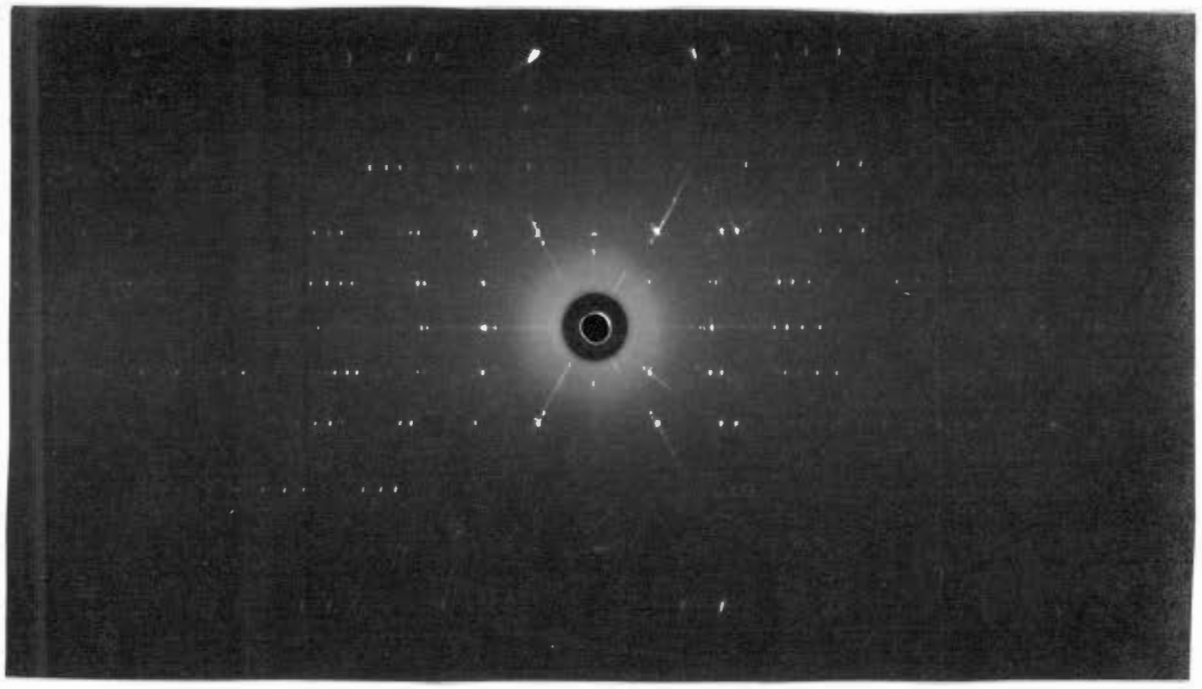

FIGURE 10. Para-methyl-iodoxy benzene.

15° oscillation photograph with the crystal rotating about the c axis, and the X-rays incident initially along the a^* axis.

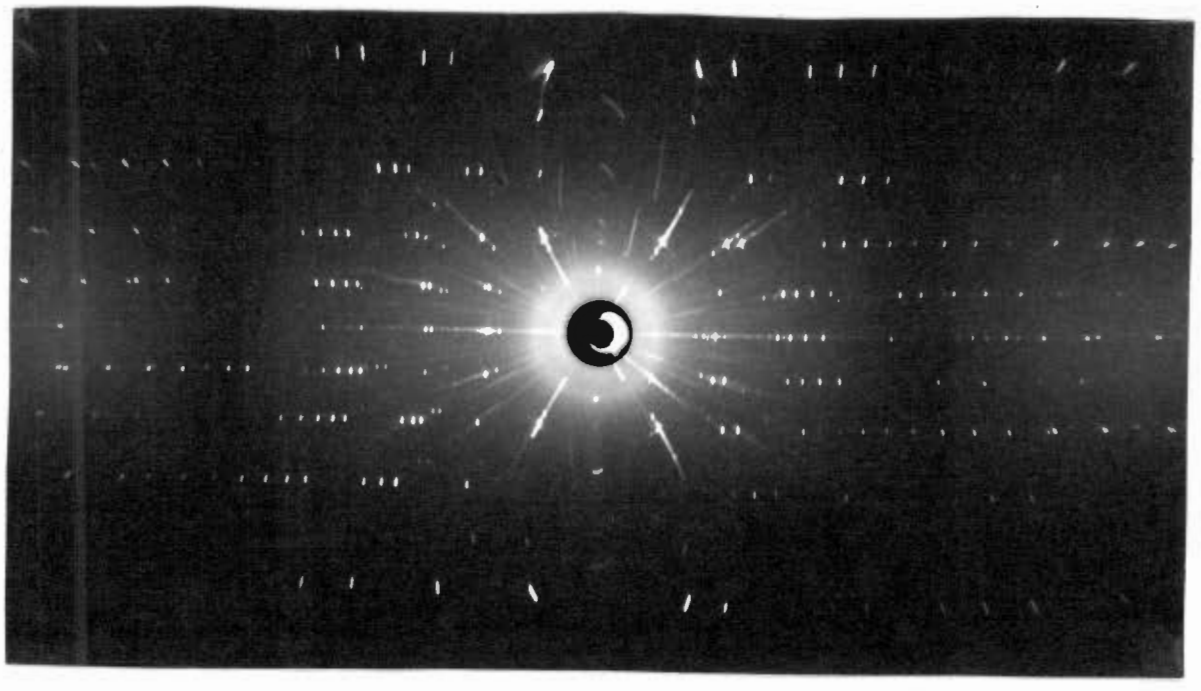

FIGURE 11. Para-chlor-iodoxy benzene.

15° oscillation photograph with the crystal rotating about the c axis, and the X-rays incident initially along the a^* axis.

THE UNIT CELL AND SPACE GROUP OF PARA-CHLOR-IODOXY BENZENE.

The unit cell, as determined from rotation photographs with CuK_α radiation, has the dimensions

$$\underline{a} = 14.4A$$

$$\underline{b} = 6.50A$$

$$\underline{c} = 8.11A$$

$$\beta = 98\tfrac{1}{2}^\circ$$

The monoclinic angle, β, was determined from a Weissenberg zero layer line photograph about the $\underline{b}$ axis.

The density of the crystal, determined by the method of flotation, is about 2.4grms./c.c., which corresponds to 4 molecules of $ClC_6H_4IO_2$ in a unit cell having the dimensions given above.

General reflections $\underline{hkl}$ of all types occur, showing that the unit cell is primitive. Reflections $\underline{hk}0$ and $0\underline{kl}$ occur with no restrictions, while $\underline{h}0\underline{l}$ spectra occur only with $\underline{l}=2n$, and spectra $0\underline{k}0$ occur only with $K=2n$. The space group is thus $P2_1/c$.

INTENSITY MEASUREMENTS.

All the observations were photographic, and were made with a cylindrical oscillation camera with CuK_α radiation filtered through nickel foil. Complete sets of rotation photographs were taken about the $\underline{a}$, $\underline{b}$, and $\underline{c}$ axes in order to get all possible $\underline{hkl}$ spectra. The intensities of the spectra were measured by comparing them visually with a calibrated scale of spots of different exposures. These intensities are, of course, on an arbitrary scale but they can be expressed on an approximately absolute scale by the use of a suitable multiplication factor.

Nearly 800 spectra were measured and used in the various projections. Table 4 gives the F values of all the observed spectra.

TABLE 6 . $F_{observed}$ and $F_{calculated}$ (for I and Cl only).

Spectrum	F(obs)	F(calc)/4	Spectrum	F(obs)	F(calc)/4
100	74	+34.2	430	26	+38.8
200	59	+51.3	530	16	+26.5
300	36	+21.3	630	15	+33.6
400	9	+12.8	730	10	+20.7
500	4	+ 0.9	12,30	7	-22.5
600	16	-22.8	13,30	9	-17.1
700	17	-16.9	14,30	10	-26.9
800	23	-41.5	15,30	9	-19.6
900	15	-25.6			
10,00	21	-40.0	140	18	+23.5
11,00	9	-24.1	240	18	+25.3
12,00	5	-23.1	340	9	+13.9
13,00	5	-14.4	440	7	+ 7.2
			640	9	-12.1
020	40	-50.4	740	5	-13.7
040	13	+22.9	840	5	-24.5
060	abs	- 0.9			
			250	7	-14.4
002	45	+11.9	350	7	-17.3
004	61	-41.0	450	10	-22.2
006	19	-21.6	550	7	-20.1
008	5	+13.7	650	5	-20.3
00,10	4	+18.9			
			160	4	+ 2.4
110	48	-10.4	560	5	- 1.8
210	87	-38.5			
310	40	-26.6	011	abs	- 5.7
410	62	-54.7	012	101	+30.4
510	24	-31.6	013	17	- 4.5
610	40	-44.9	014	26	+21.0
710	13	-24.2	015	9	- 2.0
810	10	-19.2	016	9	-10.1
910	4	- 8.9	017	9	+ 3.4
10,10	4	+ 8.6	018	9	-24.1
11,10	5	+ 7.0			
12,10	9	+28.2	021	47	-12.6
13,10	5	+18.3	022	15	-11.8
14,10	7	+32.9	023	26	-15.9
15,10	5	+22.0	024	36	+35.9
			026	10	+25.1
120	51	-30.4	027	5	+11.8
220	71	-40.8			
320	21	-18.6	031	17	+ 7.6
420	22	-10.9	032	67	-26.8
620	14	+19.3	033	9	+ 1.6
720	7	+15.8	034	22	-17.7
820	11	+36.6	035	21	- 9.1
920	9	+24.0	038	5	+20.9
10,20	11	+35.6			
11,20	7	+22.5	041	10	+17.7
12,20	5	+21.0	042	11	+ 7.4
16,20	7	-17.2	043	22	+24.2
17,20	5	-22.5	044	7	-23.8
			051	21	-12.2
130	11	+ 9.0			
230	22	+26.3			
330	22	+22.8			

TABLE 6. (continued)

Spectrum	F(obs)	F(calc)/4	Spectrum	F(obs)	F(calc)/4
061	5	-18.7	306	14	-36.9
063	15	-26.8	406	5	-16.9
			506	4	-20.9
071	14	+14.3	806	5	+ 8.0
			906	9	+23.2
102	105	+64.9	10,06	5	+16.5
202	26	+26.9	11,06	4	+31.5
302	33	+53.6			
402	20	+30.8	$10\bar{6}$	15	-20.3
502	26	+46.7	$20\bar{6}$	11	-10.5
602	13	+22.7	$30\bar{6}$	9	- 4.3
702	13	+21.7	$40\bar{6}$	9	+ 4.8
902	5	- 7.3	$50\bar{6}$	14	+27.9
10,02	5	-77.6	$60\bar{6}$	15	+18.5
11,02	7	-28.2	$70\bar{6}$	21	+36.5
12,02	5	-18.2	$80\bar{6}$	17	+24.7
13,02	7	-34.3	$90\bar{6}$	17	+28.8
14,02	5	-30.6	$10,0\bar{6}$	11	+21.2
			$12,0\bar{6}$	5	+ 9.7
$10\bar{2}$	29	-23.7			
$20\bar{2}$	10	- 7.8	208	5	- 8.6
$30\bar{2}$	61	-38.4	308	5	-14.3
$40\bar{2}$	30	-25.0	408	7	-26.5
$50\bar{2}$	59	-52.1	508	4	-19.1
$60\bar{2}$	29	-30.8	608	4	-32.0
$70\bar{2}$	28	-41.7	708	4	-16.6
$80\bar{2}$	12	-24.3			
$90\bar{2}$	9	-16.5	$10\bar{8}$	5	+ 9.8
$11,0\bar{2}$	9	+10.4	$20\bar{8}$	5	+29.9
$13,0\bar{2}$	7	+28.2	$30\bar{8}$	9	+19.9
$14,0\bar{2}$	5	+18.3	$40\bar{8}$	11	+32.8
$15,0\bar{2}$	7	+30.0	$50\bar{8}$	12	+22.4
			$60\bar{8}$	13	+21.1
104	13	-14.9	$70\bar{8}$	15	+16.0
304	4	+ 9.2	$80\bar{8}$	4	+ 5.6
404	9	+15.5			
504	10	+16.3	$10,\bar{10}$	4	+26.3
604	13	+35.8	$20,\bar{10}$	4	+18.0
704	12	+23.3	$30,\bar{10}$	4	+12.3
804	9	+38.8	$40,\bar{10}$	4	+ 9.7
904	9	+20.9			
10,04	7	+25.0	111	17	- 3.4
			211	46	-14.3
$10\bar{4}$	33	-27.0	311	25	- 6.6
$20\bar{4}$	7	-48.5	411	7	- 7.4
$30\bar{4}$	39	-28.8	811	4	- 4.3
$40\bar{4}$	33	-33.6			
$50\bar{4}$	25	-19.2	$11\bar{1}$	70	-20.2
$60\bar{4}$	18	- 5.7	$21\bar{1}$	7	- 5.1
$70\bar{4}$	9	- 2.6	$31\bar{1}$	7	- 3.2
$80\bar{4}$	7	+21.0	$41\bar{1}$	13	+ 2.7
$90\bar{4}$	9	+13.6	$51\bar{1}$	19	+ 3.0
$10,0\bar{4}$	10	+25.1	$61\bar{1}$	14	+ 5.6
$11,0\bar{4}$	5	+23.2	$71\bar{1}$	5	+ 2.0
$12,0\bar{4}$	7	+32.7	$81\bar{1}$	4	+ 2.8
$13,0\bar{4}$	7	+23.4	$91\bar{1}$	5	+ 6.4
$14,0\bar{4}$	5	+17.4	$14,1\bar{1}$	5	- 2.5
106	21	-37.0	112	103	+47.3
206	18	-23.6	212	13	+15.6

TABLE 6. (continued)

Spectrum	F(obs)	F(calc)/4	Spectrum	F(obs)	F(calc)/4
512	9	-16.5	115	27	+ 4.6
612	13	-18.5	215	7	+ 3.7
712	21	-37.9	915	4	- 5.2
812	11	-24.8			
912	14	-39.8	$11\bar{5}$	7	+ 7.6
10,12	7	-21.4	$21\bar{5}$	4	+ 2.0
11,12	5	-25.8	$31\bar{5}$	9	+ 4.2
16,12	4	+12.0	$41\bar{5}$	4	+ 2.0
			$61\bar{5}$	4	- 5.7
$11\bar{2}$	105	-56.6	$81\bar{5}$	5	- 2.7
$21\bar{2}$	57	-34.7	13,15	5	- 2.7
$31\bar{2}$	57	-38.5	14,15	7	- 2.5
$41\bar{2}$	19	-23.1			
$51\bar{2}$	7	- 6.5	116	5	-16.8
$61\bar{2}$	5	- 4.9	216	5	+ 7.3
$71\bar{2}$	11	+23.0	316	9	+ 6.0
$81\bar{2}$	7	+14.8	416	7	+20.6
$91\bar{2}$	15	+37.5	516	7	+25.5
10,12	9	+25.5	616	7	+24.4
11,12	12	+34.4	716	7	+33.2
12,12	7	+25.6	816	5	+18.2
13,12	5	+18.2	916	5	+26.1
17,12	7	-18.5			
			$11\bar{6}$	16	+32.4
113	7	+12.8	$21\bar{6}$	18	+25.7
213	7	- 3.0	$31\bar{6}$	25	+33.2
313	7	- 3.1	$41\bar{6}$	24	+30.2
11,13	9	- 6.5	$51\bar{6}$	20	+21.1
			$61\bar{6}$	13	+21.8
$11\bar{3}$	19	+ 2.5	$71\bar{6}$	10	+ 2.4
$21\bar{3}$	9	+ 5.6	$91\bar{6}$	7	-18.4
$41\bar{3}$	13	+ 8.5	10,16	5	-14.2
$51\bar{3}$	13	+ 3.1	11,16	5	-27.4
$61\bar{3}$	5	+ 2.9	12,16	5	-26.0
$91\bar{3}$	5	- 1.6			
12,13	5	+ 2.7	$51\bar{7}$	5	- 2.3
			$61\bar{7}$	5	- 6.6
114	43	+32.8	$71\bar{7}$	9	- 2.4
214	53	+30.4			
314	23	+42.2	118	7	- 26.0
414	19	+24.1	218	7	-28.2
514	10	+34.4	718	5	+13.9
614	7	+10.3			
814	5	- 5.0	$11\bar{8}$	7	+25.9
914	5	-11.2	$21\bar{8}$	7	+ 9.6
10,14	9	-22.7	$31\bar{8}$	5	+14.2
11,14	9	-19.0	$41\bar{8}$	5	- 8.1
			$81\bar{8}$	9	-24.6
$11\bar{4}$	21	-15.8	$91\bar{8}$	5	-28.4
$21\bar{4}$	9	+ 7.6	10,18	4	-17.7
$31\bar{4}$	4	+ 3.9	11,18	4	-23.7
$41\bar{4}$	24	+32.2			
$51\bar{4}$	18	+24.1	121	4	- 3.2
$61\bar{4}$	23	+39.9	221	11	- 6.0
$71\bar{4}$	17	+30.6	321	5	+10.2
$81\bar{4}$	21	+29.8	421	5	+ 3.5
$91\bar{4}$	9	+26.4	521	16	+12.8
10,14	5	+ 9.3	621	13	+10.6
11,14	5	+11.8			

TABLE 6. (continued)

Spectrum	F(obs)	F(calc)/4	Spectrum	F(obs)	F(calc)/4
721	9	+ 9.8	$52\bar{3}$	7	- 6.1
821	7	+12.4	$62\bar{3}$	4	- 7.2
921	5	+ 3.6	$72\bar{3}$	5	- 7.3
10,21	5	+ 8.9	$82\bar{3}$	5	-13.2
			$92\bar{3}$	5	- 5.8
$12\bar{1}$	74	+15.6	10,$2\bar{3}$	5	-13.0
$22\bar{1}$	55	+12.9			
$32\bar{1}$	32	+15.5	124	15	+12.1
$42\bar{1}$	20	+ 7.9	324	9	- 3.5
$52\bar{1}$	13	+14.6	424	7	-10.6
$72\bar{1}$	7	+ 7.3	524	7	-18.3
$92\bar{1}$	5	- 2.3	624	11	-29.5
10,$2\bar{1}$	7	- 7.3	724	5	-23.1
11,$2\bar{1}$	5	- 9.6	824	9	-34.7
12,$2\bar{1}$	5	- 6.6	924	5	-18.7
13,21	5	-12.0	10,24	5	-24.9
			11,24	5	- 8.3
122	51	-26.6			
222	41	-26.3	$12\bar{4}$	41	+26.0
322	44	-44.4	$22\bar{4}$	46	+39.7
422	25	-28.3	$32\bar{4}$	35	+29.7
522	27	-40.8	$42\bar{4}$	28	+21.4
622	13	-20.0	$52\bar{4}$	13	+20.9
722	5	-20.8	$82\bar{4}$	7	-19.1
822	5	- 5.4	$92\bar{4}$	5	-13.6
10,22	7	+ 8.7	10,$2\bar{4}$	5	-29.8
11,22	5	+24.5	11,$2\bar{4}$	4	-24.5
12,22	5	+17.8	12,$2\bar{4}$	5	-26.9
13,22	5	+31.4	13,$2\bar{4}$	4	-24.7
15,22	4	+24.5			
			125	5	- 7.1
$12\bar{2}$	13	+ 4.6	325	7	-12.5
$22\bar{2}$	18	+ 7.4	425	10	-5.7
$32\bar{2}$	34	+32.8	525	5	-13.0
$42\bar{2}$	25	+23.2	625	5	- 7.6
$52\bar{2}$	44	+43.7			
$62\bar{2}$	18	+29.3	$22\bar{5}$	7	- 5.7
$72\bar{2}$	14	+34.7	$32\bar{5}$	12	-10.8
$82\bar{2}$	10	+23.9	$42\bar{5}$	12	- 6.3
$92\bar{2}$	7	+13.2	$52\bar{5}$	10	-14.3
10,$2\bar{2}$	5	+10.1	$62\bar{5}$	10	- 4.7
13,$2\bar{2}$	7	-25.1	$72\bar{5}$	10	-11.5
14,$2\bar{2}$	5	-18.4	$82\bar{5}$	4	- 2.1
15,$2\bar{2}$	9	-27.8	$92\bar{5}$	4	- 5.6
16,$2\bar{2}$	9	-22.5			
17,22	5	-19.0	126	11	+29.0
			226	10	+25.3
123	11	-9.4	326	9	+32.0
223	11	-11.8	526	7	+21.4
323	15	-10.4	826	5	-13.1
723	5	+ 3.7	926	5	-17.1
823	5	+10.7			
10,23	7	+ 9.9	$12\bar{6}$	10	+13.5
13,23	7	+ 8.6	$22\bar{6}$	10	+13.9
			$32\bar{6}$	9	- 7.6
$12\bar{3}$	32	+ 4.0	$52\bar{6}$	9	-24.2
$22\bar{3}$	17	+12.4	$62\bar{6}$	10	-20.1
$32\bar{3}$	9	+ 2.4	$72\bar{6}$	11	-29.3
$42\bar{3}$	7	+ 3.0	$88\bar{6}$	10	-27.6

TABLE 6. (continued)

Spectrum	F(obs)	F(calc)/4	Spectrum	F(obs)	F(calc)/4
$9\bar{2}6$	7	-21.7	$13\bar{2}$	67	+39.9
$10,\bar{2}6$	5	-23.5	$23\bar{2}$	38	+27.4
			$33\bar{2}$	38	+28.5
827	5	-15.1	$43\bar{2}$	20	+17.8
			$53\bar{2}$	5	+5.7
$12\bar{7}$	5	- 4.4	$63\bar{2}$	4	+ 2.0
$22\bar{7}$	5	-12.4	$73\bar{2}$	7	-16.9
$32\bar{7}$	7	- 3.6	$83\bar{2}$	5	-13.8
$42\bar{7}$	5	- 7.2	$93\bar{2}$	7	-29.2
$62\bar{7}$	5	+ 2.2	$10,\bar{3}2$	7	-22.4
			$11,\bar{3}2$	7	-28.2
328	5	+18.9	$12,\bar{3}2$	7	-21.4
428	4	+18.7	$13,\bar{3}2$	9	-15.9
528	4	+23.0	$14,\bar{3}2$	5	-12.9
628	5	+25.9			
			233	11	+12.1
$22\bar{8}$	9	-24.4	333	13	+ 3.1
$32\bar{8}$	5	-23.6	433	12	+18.2
$42\bar{8}$	9	-24.5	533	11	+11.1
$52\bar{8}$	9	-26.8	633	12	+15.6
$62\bar{8}$	9	-14.4	733	7	+14.1
$72\bar{8}$	5	-18.4	833	5	+ 7.1
			13,33	4	- 5.1
131	28	+20.4	14,33	4	-11.6
231	44	+17.1			
331	32	+13.8	$13\bar{3}$	21	-12.0
431	17	+17.6	$23\bar{3}$	24	-13.9
531	10	+ 2.7	$33\bar{3}$	28	-12.7
631	5	+10.3	$43\bar{3}$	21	-20.8
731	7	- 7.5	$53\bar{3}$	12	- 8.3
931	5	-12.7	$63\bar{3}$	7	-18.1
10,31	5	-10.8	$83\bar{3}$	5	- 7.4
11,31	7	-11.8	$12,\bar{3}3$	5	+14.7
12,31	9	-15.4	$13,\bar{3}3$	5	+ 7.5
13,31	5	- 6.4	$14,\bar{3}3$	5	+16.8
$13\bar{1}$	17	+17.5	134	13	-23.0
$43\bar{1}$	11	-11.4	234	12	-31.5
$53\bar{1}$	7	- 7.6	334	9	-24.3
$63\bar{1}$	12	-14.0	434	9	-31.9
$73\bar{1}$	10	-17.1	534	5	-16.1
$83\bar{1}$	7	-10.8	634	5	-18.6
$93\bar{1}$	5	-18.3	10,34	4	+18.9
$10,\bar{3}1$	5	- 3.1	11,34	4	+17.7
$11,\bar{3}1$	5	-11.0			
$13,\bar{3}1$	5	+ 2.0	$13\bar{4}$	10	+11.8
$14,\bar{3}1$	5	+ 6.7	$33\bar{4}$	7	- 2.3
$16,\bar{3}1$	7	+ 7.5	$43\bar{4}$	19	-24.2
			$53\bar{4}$	12	-19.6
132	31	-33.2	$63\bar{4}$	10	-31.5
232	9	-14.0	$73\bar{4}$	9	-25.8
332	5	-11.9	$83\bar{4}$	7	-24.8
532	9	+12.8	$93\bar{4}$	5	-21.4
632	11	+16.0			
732	13	+29.2	135	10	-16.8
832	7	+21.9	235	5	-10.1
932	7	+21.5	735	5	+13.9
10,32	7	+27.6			
11,32	5	+16.1			

TABLE 6. (continued)

Spectrum	F(obs)	F(calc)/4
135	15	-19.6
235	15	- 5.3
335	17	-13.3
435	5	- 1.3
635	5	+ 4.8
735	4	+11.4
835	4	+ 7.3
436	5	-17.0
536	5	-20.8
636	7	-21.3
736	5	-27.2
136	5	-25.9
236	7	-22.4
336	12	-27.5
436	12	-25.4
536	9	-17.3
636	7	-17.3
237	5	-15.4
337	5	- 6.5
537	5	- 7.7
437	5	+15.0
537	7	+ 6.9
637	5	+17.6
737	5	+ 4.2
238	4	+23.6
238	5	- 9.4
141	10	+ 3.3
241	9	+ 7.5
341	11	-14.5
441	15	- 6.3
541	16	-19.8
641	11	-17.2
741	9	-19.9
841	7	-12.0
941	5	-18.0
13,41	9	+10.6
14,41	7	+ 9.0
141	17	-13.8
241	26	-19.6
341	23	-23.1
441	23	-12.9
541	18	-22.0
641	7	- 3.5
741	5	-11.1
10,41	5	+12.4
11,41	5	+16.5
12,41	7	+11.9
13,41	7	+20.5
15,41	5	+15.5
142	12	+17.7
242	12	+20.1
342	12	+29.0
442	7	+22.7
542	9	+27.2
642	7	+16.3
13,42	7	-23.0
142	10	+ 2.3
342	7	-20.2
442	11	-18.9
542	19	-28.9
642	9	-23.1
742	9	-24.6
842	7	-18.0
13,42	7	+17.8
143	23	+22.8
243	23	+17.0
343	14	+16.5
443	5	+5.7
843	5	-16.8
943	7	-10.3
10,43	7	-17.0
11,43	7	-16.0
12,43	4	-10.4
143	21	- 8.3
243	18	-18.5
343	5	- 2.4
443	5	- 3.4
543	9	+ 9.5
643	9	+11.8
743	9	+12.6
843	9	+21.8
943	9	+10.7
10,43	7	+21.7
11,43	5	+ 5.4
12,43	5	+12.1
14,43	4	- 2.6
244	17	- 9.9
144	7	-21.2
244	9	-27.4
344	5	-22.4
444	5	-19.2
544	4	-14.7
145	5	+11.4
245	7	+ 2.1
345	9	+20.7
445	7	+10.5
545	5	+21.8
645	4	+13.3
445	7	+11.4
545	7	+23.5

TABLE 6. (continued)

Spectrum	F(obs)	F(calc)/4	Spectrum	F(obs)	F(calc)/4
146	4	-22.1	154	4	+16.2
246	5	-20.7	254	4	+20.0
346	4	-23.1			
			25$\bar{4}$	5	- 3.0
24$\bar{6}$	4	- 9.1			
			15$\bar{5}$	4	+25.6
147	4	- 8.7	35$\bar{5}$	4	+17.1
14$\bar{7}$	4	+ 9.4	157	4	+ 2.3
24$\bar{7}$	4	+20.9	357	5	+ 2.0
34$\bar{7}$	5	+ 6.9			
44$\bar{7}$	4	+12.2	55$\bar{7}$	5	- 1.6
151	29	-24.6	161	5	+ 1.5
251	26	-21.6	261	9	- 6.7
351	20	-18.1	361	5	+14.9
451	10	-21.6	461	10	+8.6
551	5	- 5.0	561	10	+22.2
851	5	+ 4.1	661	10	+20.4
951	7	+16.8	761	9	+19.8
10,51	9	+15.2	861	5	+23.2
11,51	10	+16.7			
12,51	4	+21.1	16$\bar{1}$	17	+16.2
			26$\bar{1}$	18	+22.1
15$\bar{1}$	20	-20.4	36$\bar{1}$	17	+25.5
25$\bar{1}$	9	- 2.9	46$\bar{1}$	14	+16.2
45$\bar{1}$	7	+13.4	56$\bar{1}$	11	+23.8
55$\bar{1}$	7	+10.6	66$\bar{1}$	5	+ 4.7
65$\bar{1}$	12	+18.4	96$\bar{1}$	4	- 5.8
75$\bar{1}$	13	+22.3	10,6$\bar{1}$	4	-14.8
85$\bar{1}$	9	+15.3	11,6$\bar{1}$	4	-19.8
95$\bar{1}$	5	+24.0			
			163	13	-18.8
152	5	+18.7	263	9	-21.8
252	5	+11.4	363	5	-18.9
			463	5	- 7.9
15$\bar{2}$	7	-22.9			
25$\bar{2}$	5	-19.6	16$\bar{3}$	4	+11.1
35$\bar{2}$	7	-17.5	26$\bar{3}$	9	+19.8
45$\bar{2}$	7	-20.7	36$\bar{3}$	5	- 1.8
			66$\bar{3}$	5	-14.0
153	13	+ 6.4	76$\bar{3}$	5	-15.7
253	7	-14.5	86$\bar{3}$	4	-25.0
353	7	- 5.4	96$\bar{3}$	5	-14.4
453	9	-23.3	10,6$\bar{3}$	5	-24.6
553	9	-15.6			
653	5	-21.1	165	4	- 2.4
753	5	-19.1	565	4	-25.1
15$\bar{3}$	10	+15.1	46$\bar{5}$	4	-14.9
25$\bar{3}$	14	+17.7	56$\bar{5}$	4	-26.8
35$\bar{3}$	18	+17.0			
45$\bar{3}$	15	+26.4	171	14	+25.0
55$\bar{3}$	12	+12.0	271	14	+22.8
65$\bar{3}$	13	+22.9	371	10	+19.7
75$\bar{3}$	7	+ 3.4	471	9	+21.8
12,5$\bar{3}$	4	-20.0	571	4	+ 6.6
13,5$\bar{3}$	4	-11.7			

TABLE 6. (continued)

Spectrum	F(obs)	F(calc)/4
$17\bar{1}$	5	+19.5
$27\bar{1}$	7	+ 2.4
$57\bar{1}$	4	-11.8
$67\bar{1}$	5	-19.5
$77\bar{1}$	4	-23.7
$87\bar{1}$	5	-17.9
$97\bar{1}$	4	-24.6
$37\bar{2}$	4	- 1.8
$47\bar{2}$	4	- 3.8
173	4	- 5.8
273	4	+13.6
373	4	+ 7.7
473	5	+23.4
$17\bar{3}$	4	-15.5
$27\bar{3}$	5	-19.0
$37\bar{3}$	7	-19.2
$47\bar{3}$	7	-26.9
$57\bar{3}$	4	-15.1
$67\bar{3}$	4	-22.8
$18\bar{1}$	4	-17.0
$28\bar{1}$	5	-22.1
$38\bar{1}$	5	-24.6

PATTERSON-HARKER PROJECTIONS.

The distances of atoms from a glide plane parallel to the b axis and with translation c/2 may be determined by Harker's method, by evaluating the Patterson series

$$P(u,v,w) = \frac{1}{V} \sum_{h=-\infty}^{+\infty} \sum_{k} \sum_{l} |F(hkl)|^2 \cos 2\pi \left(h\frac{u}{a} + k\frac{v}{b} + l\frac{w}{c} \right)$$

for the line u = 0, w = c/2. This gives

$$P(0,v,c/2) = \sum_{k=-\infty}^{+\infty} B(k) \cos 2\pi \frac{kv}{b}$$

where $$B(k) = \sum_{h=-\infty}^{+\infty} \sum_{l} (-1)^l |F(hkl)|^2$$

The distance of the maxima in P along this line from the origin gives twice the distance of the corresponding atom from the glide plane. This distribution is shown in fig.12 where the maxima are determined almost entirely by the iodine atom.

To obtain the distances of the atoms from a two-fold screw axis parallel to b, P(u,v,w) is evaluated for the plane v = b/2. This gives

$$P(u,\frac{b}{2},w) = \sum_{h=-\infty}^{+\infty} \sum_{l} C(hl) \cos 2\pi \left(h\frac{u}{a} + l\frac{w}{c} \right)$$

where $$C(hl) = \sum_{k=-\infty}^{+\infty} (-1)^k |F(hkl)|^2$$

This distribution is shown in fig.13, together with a key diagram fig.14.

The largest peak labelled A, in fig.14, is the only "space group" peak, its vector distance from the origin being twice the vector distance of the iodine atom from the screw axis. The peak B appears because the iodine atoms of molecules II and III in figs.19, 20, and 21 although not derived from one

(pages 58, 59, 60)

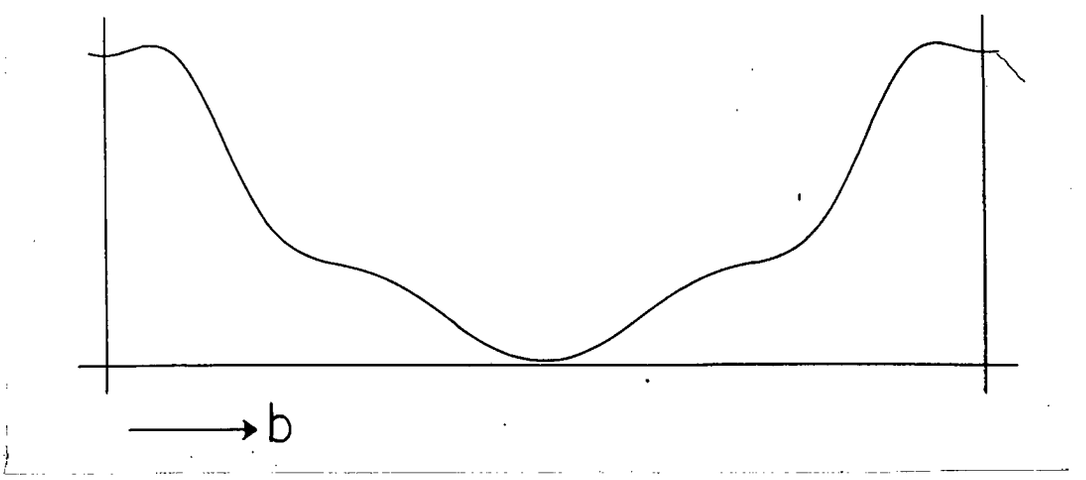

FIGURE 12. The Patterson-Harker distribution P(0,v,c/2), in which the distance of a maximum from the origin is twice the distance of the corresponding atom from the glide plane.

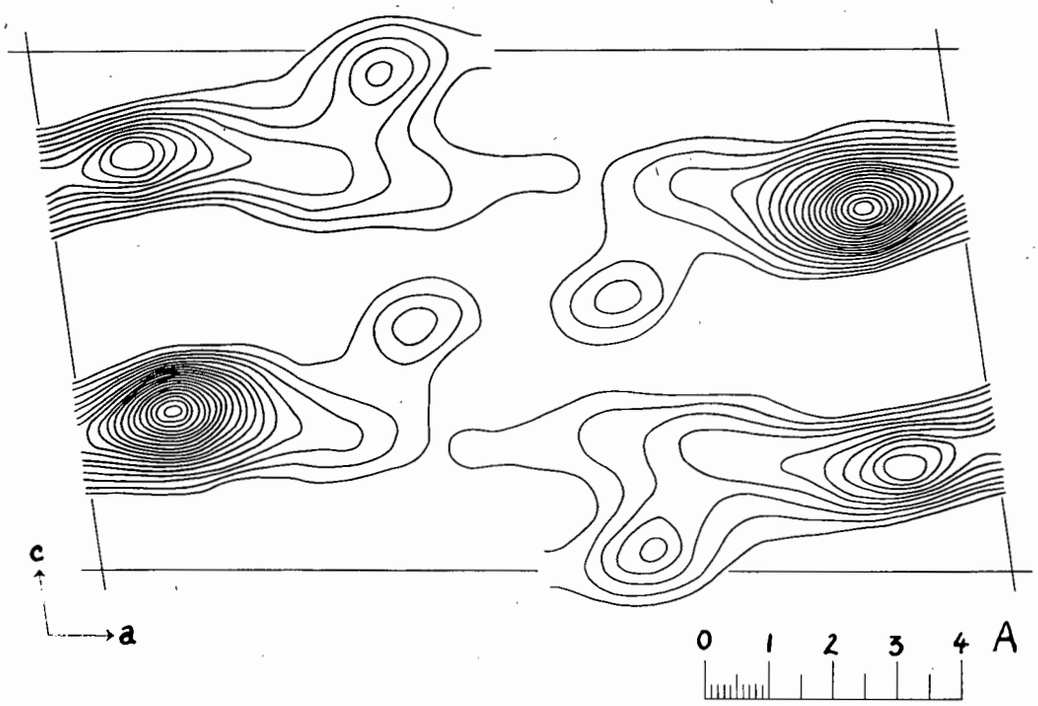

FIGURE 13. The Patterson-Harker distribution P(u,b/2,w), in which the distance of a maximum from the origin gives twice vector distance parallel to the ac plane between atoms which have a vector separation parallel to b of b/2.

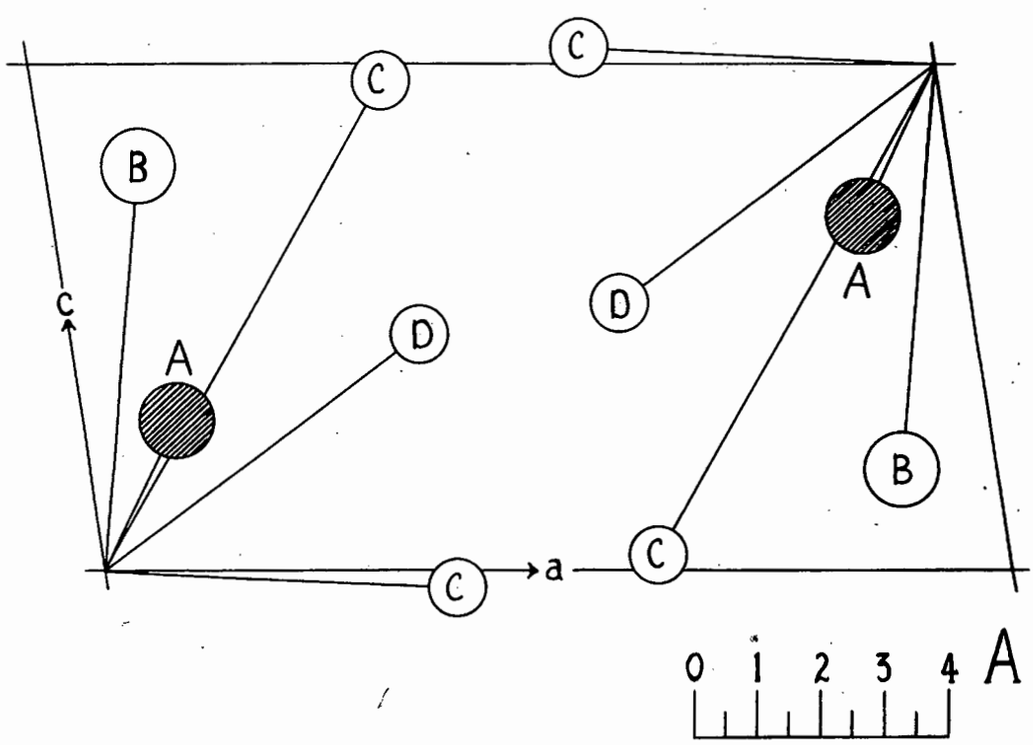

FIGURE 14. Key diagram to fig.13.

another by the operation of the two-fold screw axis have a vector separation parallel to b near enough to b/2 for a peak to appear in the Patterson-Harker distribution P(u,b/2,w).

The peak C appears because the iodine and chlorine atoms in the same molecule have a vector separation parallel to b of very nearly b/2, and peak D appears because the iodine atoms of molecule I and the chlorine atom of molecule II have a vector separation parallel to b near enough to b/2 for a peak to appear in the Patterson-Harker distribution P(u, b/2, w).

The Patterson-Harker projections have thus fixed, not only the positions of the iodine atoms, but have given approximate positions to the chlorine atoms also. These coordinates were then used to calculate structure factors for the two-dimensional Fourier projections on the planes (001) and (010).

CALCULATION OF STRUCTURE FACTORS.

In the space group $P2_1/c$ the coordinates of equivalent point positions are

$$(x,y,z),\ (\bar{x},\bar{y},\bar{z}),\ (x,\tfrac{1}{2}-y,z+\tfrac{1}{2}),\ (\bar{x},y+\tfrac{1}{2},\tfrac{1}{2}-z).$$

The general structure factor is given by

$$F(hkl) = \sum_s f_s (A_s + iB_s)$$

where for $k+l = 2n$ $\begin{cases} A = 4\cos 2\pi(hx+lz)\cos 2\pi ky \\ B = 0 \end{cases}$

and for $k+l = 2n+1$ $\begin{cases} A = -4\sin 2\pi(hx+lz)\sin 2\pi ky \\ B = 0 \end{cases}$

f_s is the atomic scattering factor of the atom s in the unit cell, whose coordinates are (x_s, y_s, z_s) and the summation was taken for the I and Cl atoms only. The atomic scattering factors used were those given in "Internationale Tabellen zur Bestimmung von Kristallstrukturen" volume 2, without the

application of any temperature factor. Consequently all the high order calculated F values are much too large, but this was immaterial as the only reason for calculating F values was to give appropriate signs to the observed F values, since the crystal has a centre of symmetry at the origin. Table 6 gives the observed and calculated F values used in computing the three-dimensional Fourier sections.

TWO-DIMENSIONAL FOURIER SYNTHESES.

In order to check the coordinates of the iodine and chlorine atoms obtained from the Patterson-Harker distributions, and to get some idea of the positions of the oxygen atoms and the benzene ring, two-dimensional Fourier projections of the structure were made on the planes (001) and (010) using spectra of the type hk0 and h0l respectively. These projections were made using the method of Lipson and Beevers (1936), and are shown in figs. 15 and 16.

It was found that the y coordinate of the iodine atom was not quite that given by the Patterson-Harker distribution given in fig. 12, in which the distance of the maximum from the origin was taken to represent twice the distance, parallel to b, of the iodine atom from the glide plane. As this distribution is symmetrical about the origin the peaks are unresolved from each other resulting in a displacement of the maxima in the distribution P(0,v,c/2).

The two-dimensional projections also gave more accurate coordinates for the chlorine atom and showed the region of the benzene ring, but it was impossible to locate the oxygen atoms in the region near the iodine atom.

It was decided, therefore, to determine the structure by means of three-dimensional Fourier sections parallel to the ab plane as suggested by Booth (1945).

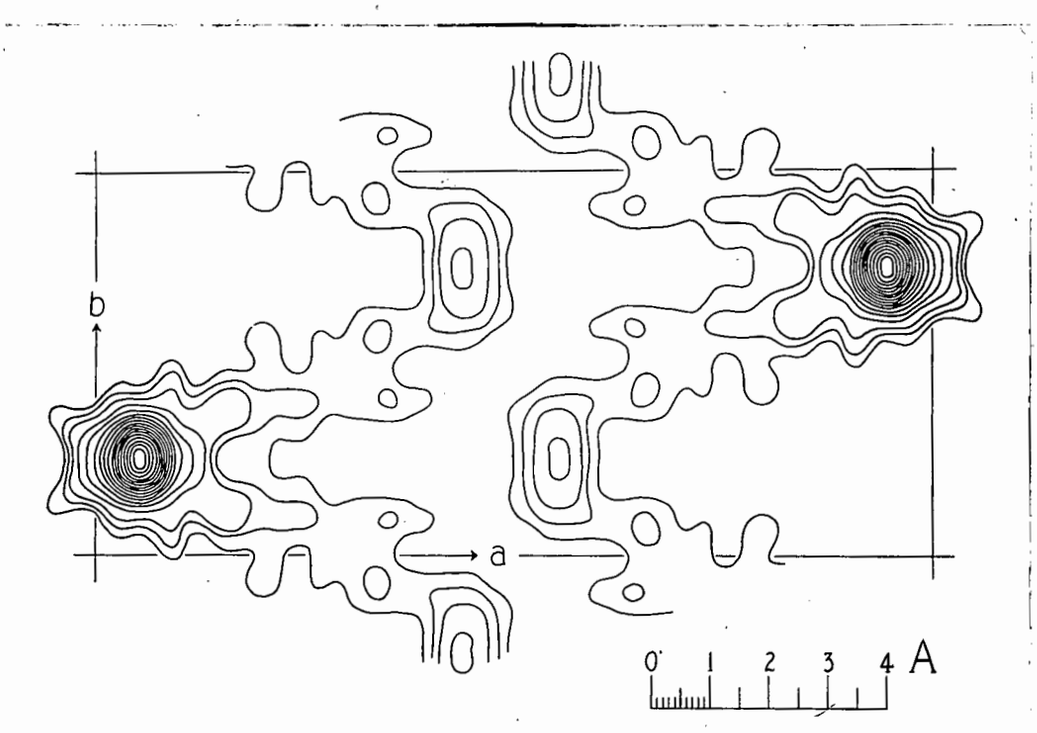

FIGURE 15. Fourier projection of the structure in the c direction on to the ab plane.

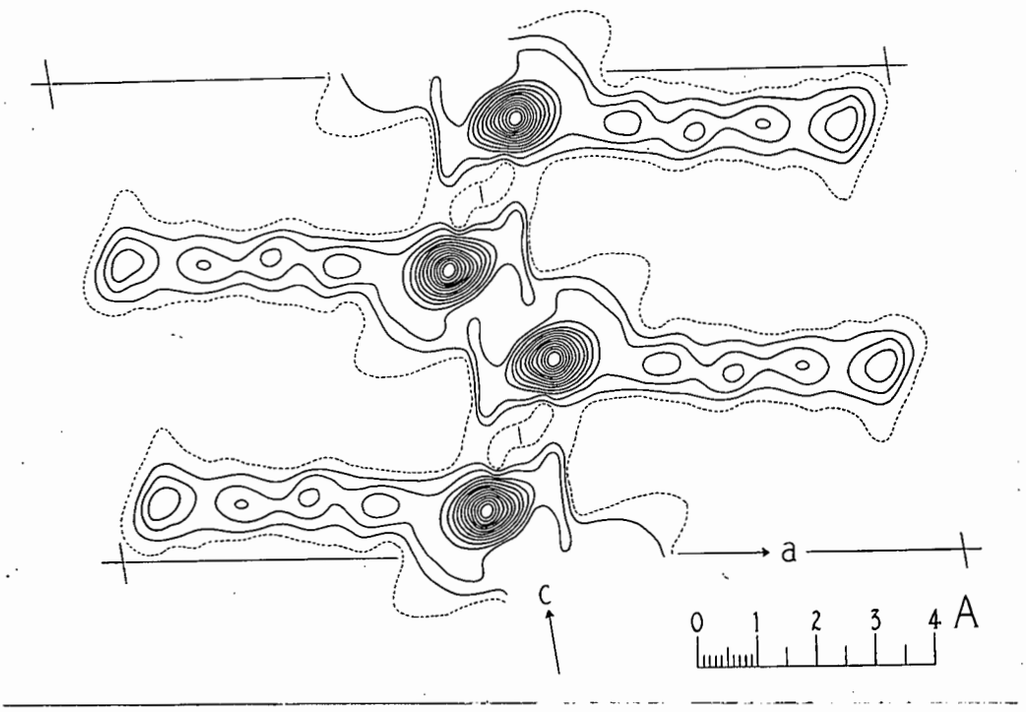

FIGURE 16. Fourier projection of the structure in the b direction on to the ac plane.

For this, all the structure factors F(hkl) were required. The signs were obtained by calculating the structure factors for the iodine and chlorine atoms only. In this way not more than 10 or 15 spectra out of nearly 800 used would have the wrong sign, and these, having very small F values, would have a negligible effect on the positions of the centres of the peaks. A table of F(observed) and F(calculated), (for the iodine and chlorine atoms only) is given in Table 6 .

THREE-DIMENSIONAL FOURIER SECTIONS.

The electron density in a plane of crystal at $z = z_1$ is given by

$$\rho(x,y,z_1) = \frac{1}{V(abc)} \sum_{h}^{+\infty} \sum_{k}^{+\infty} \sum_{\ell}^{+\infty} F(hk\ell) \exp\left[-2\pi i\left(\frac{hx}{a} + \frac{ky}{b} + \frac{\ell z_1}{c}\right)\right]$$

Since the crystal has a centre of symmetry the series takes the form

$$\rho(x,y,z_1) = \frac{1}{V(abc)} \sum_{h}^{+\infty} \sum_{k}^{+\infty} \sum_{\ell}^{+\infty} \pm |F(hk\ell)| \cos 2\pi\left(\frac{hx}{a} + \frac{ky}{b} + \frac{\ell z_1}{c}\right)$$

Using an argument similar to that used by Lipson and Beevers (1936), the above expression can be put into a form suitable for the use of Lipson and Beevers strips.

$$V\rho(x,y,z_1) = \frac{1}{V} \sum_{-H}^{+H} \sum_{-K}^{+K} \sum_{-L}^{+L} F(hk\ell) \exp\left[-2\pi i\left(\frac{hx}{a} + \frac{ky}{b} + \frac{\ell z_1}{c}\right)\right.$$

$$= \sum_{-H}^{+H} \sum_{-K}^{+K} \sum_{-L}^{+L} \left\{F(hk\ell) \exp\left[-2\pi i\left(\frac{hx}{a} + \frac{ky}{b} + \frac{\ell z_1}{c}\right)\right.\right.$$

$$\left.\left. + F^*(hk\ell) \exp 2\pi i\left(\frac{hx}{a} + \frac{ky}{b} + \frac{\ell z_1}{c}\right)\right\}\right.$$

$$= \sum_{-H}^{+H} \sum_{-K}^{+K} \sum_{-L}^{+L} |F(hk\ell)| \left\{\exp\left[-2\pi i\left(\frac{hx}{a} + \frac{ky}{b} + \frac{\ell z_1}{c} - \delta\right)\right]\right.$$

$$\left. + \exp 2\pi i\left(\frac{hx}{a} + \frac{ky}{b} + \frac{\ell z_1}{c} - \delta\right)\right\}$$

$$= 2 \sum_{-H}^{+H} \sum_{-K}^{+K} \sum_{-L}^{+L} |F(hk\ell)| \cos 2\pi\left(\frac{hx}{a} + \frac{ky}{b} + \frac{\ell z_1}{c} - \delta\right)$$

$$\frac{V}{2}\rho(x,y,z_1) = \sum_{-H}^{+H}\sum_{-K}^{+K}\sum_{\#}^{+L} |F(hkl)| \cos 2\pi\left(\frac{hx}{a}+\frac{ky}{b}+\frac{lz_1}{c}-\delta\right)$$
$$+ \sum_{-H}^{+H}\sum_{-K}^{+K}\sum_{-L}^{-1} |F(hkl)| \cos 2\pi\left(\frac{hx}{a}+\frac{ky}{b}+\frac{lz_1}{c}-\delta\right)$$
$$+ \sum_{-H}^{+H}\sum_{-K}^{+K} |F(hk0)| \cos 2\pi\left(\frac{hx}{a}+\frac{ky}{b}-\delta\right)$$
$$= \sum_{1}^{H}\sum_{-K}^{+K}\sum_{1}^{L} |F(hkl)| \cos 2\pi\left(\frac{hx}{a}+\frac{ky}{b}+\frac{lz_1}{c}-\delta\right)$$
$$+ \sum_{-H}^{-1}\sum_{-K}^{+K}\sum_{1}^{L} |F(hkl)| \cos 2\pi\left(\frac{hx}{a}+\frac{ky}{b}+\frac{lz_1}{c}-\delta\right)$$
$$+ \sum_{-K}^{+K}\sum_{1}^{L} |F(0kl)| \cos 2\pi\left(\frac{ky}{b}+\frac{lz_1}{c}-\delta\right)$$
$$+ \sum_{1}^{H}\sum_{-K}^{+K}\sum_{-L}^{-1} |F(hkl)| \cos 2\pi\left(\frac{hx}{a}+\frac{ky}{b}+\frac{lz_1}{c}-\delta\right)$$
$$+ \sum_{-H}^{-1}\sum_{-K}^{+K}\sum_{-L}^{-1} |F(hkl)| \cos 2\pi\left(\frac{hx}{a}+\frac{ky}{b}+\frac{lz_1}{c}-\delta\right)$$
$$+ \sum_{-K}^{+K}\sum_{-L}^{-1} |F(hkl)| \cos 2\pi\left(\frac{ky}{b}+\frac{lz_1}{c}-\delta\right)$$
$$+ \sum_{1}^{H}\sum_{-K}^{+K} |F(hk0)| \cos 2\pi\left(\frac{hx}{a}+\frac{ky}{b}-\delta\right)$$
$$+ \sum_{-H}^{-1}\sum_{-K}^{+K} |F(hk0)| \cos 2\pi\left(\frac{hx}{a}+\frac{ky}{b}-\delta\right)$$
$$+ \sum_{-K}^{+K} |F(0k0)| \cos 2\pi\left(\frac{ky}{b}-\delta\right)$$
$$+ F(000)$$
$$= 2\left[\sum_{1}^{H}\sum_{-K}^{+K}\sum_{1}^{L} |F(hkl)| \cos 2\pi\left(\frac{hx}{a}+\frac{ky}{b}+\frac{lz_1}{c}-\delta\right)\right.$$
$$+ \sum_{1}^{H}\sum_{-K}^{+K}\sum_{-L}^{-1} |F(hkl)| \cos 2\pi\left(\frac{hx}{a}+\frac{ky}{b}+\frac{lz_1}{c}-\delta\right)$$
$$+ \sum_{-K}^{+K}\sum_{1}^{L} |F(0kl)| \cos 2\pi\left(\frac{ky}{b}+\frac{lz_1}{c}-\delta\right)$$
$$+ \sum_{1}^{H}\sum_{-K}^{+K} |F(hk0)| \cos 2\pi\left(\frac{hx}{a}+\frac{ky}{b}-\delta\right)$$
$$\left.+ \sum_{1}^{K} |F(0k0)| \cos 2\pi\left(\frac{ky}{b}-\delta\right) + \frac{F(000)}{2}\right]$$

$$
\begin{aligned}
V\rho(x,y,z_1) = {} & \sum_{1}^{H}\sum_{1}^{K}\sum_{1}^{L} |F(hkl)| \cos 2\pi\left(\frac{hx}{a}+\frac{ky}{b}+\frac{lz_1}{c}-\delta\right) \\
& + \sum_{1}^{H}\sum_{-K}^{-1}\sum_{1}^{L} |F(hkl)| \cos 2\pi\left(\frac{hx}{a}+\frac{ky}{b}+\frac{lz_1}{c}-\delta\right) \\
& + \sum_{1}^{H}\sum_{1}^{L} |F(h0l)| \cos 2\pi\left(\frac{hx}{a}+\frac{lz_1}{c}-\delta\right) \\
& + \sum_{1}^{H} |F(h00)| \cos 2\pi\left(\frac{hx}{a}-\delta\right) \\
& + \sum_{1}^{L} |F(00l)| \cos 2\pi\left(\frac{lz_1}{c}-\delta\right) \\
& + \sum_{1}^{H}\sum_{1}^{K}\sum_{-L}^{-1} |F(hkl)| \cos 2\pi\left(\frac{hx}{a}+\frac{ky}{b}+\frac{lz_1}{c}-\delta\right) \\
& + \sum_{1}^{H}\sum_{-K}^{-1}\sum_{-L}^{-1} |F(hkl)| \cos 2\pi\left(\frac{hx}{a}+\frac{ky}{b}+\frac{lz_1}{c}-\delta\right) \\
& + \sum_{1}^{H}\sum_{-L}^{-1} |F(h0l)| \cos 2\pi\left(\frac{hx}{a}+\frac{lz_1}{c}-\delta\right) \\
& + \sum_{1}^{K}\sum_{1}^{L} |F(0kl)| \cos 2\pi\left(\frac{ky}{b}+\frac{lz_1}{c}-\delta\right) \\
& + \sum_{-K}^{-1}\sum_{1}^{L} |F(0kl)| \cos 2\pi\left(\frac{ky}{b}+\frac{lz_1}{c}-\delta\right) \\
& + \sum_{1}^{H}\sum_{1}^{K} |F(hk0)| \cos 2\pi\left(\frac{hx}{a}+\frac{ky}{b}-\delta\right) \\
& + \sum_{1}^{H}\sum_{-K}^{1} |F(hk0)| \cos 2\pi\left(\frac{hx}{a}+\frac{ky}{b}-\delta\right) \\
& + \sum_{1}^{K} |F(0k0)| \cos 2\pi\left(\frac{ky}{b}-\delta\right) \\
& + \frac{F(000)}{2}
\end{aligned}
$$

The cosine terms can be expanded, and the above equation re-written with

$$|F(hkl)| \cos 2\pi\delta = C(hkl)$$

$$\text{and } |F(hkl)| \sin 2\pi\delta = S(hkl)$$

When the crystal has a centre of symmetry, $2\pi\delta = 0°$ or $180°$.

Then $C(hkl) = |F(hkl)| \cos 2\pi\delta = F(hkl)$

and $S(hkl) = |F(hkl)| \sin 2\pi\delta = 0.$

When these steps have been carried out, the equation is of the same form as before, but with $F(hkl)$ substituted for $|F(hkl)|$ and all the δ.s left out.

The equation can then be written in the form:

$$V\rho(x,y,z_i) = \alpha + \sum_1^K \beta \cos 2\pi \frac{ky}{b} - \sum_1^K \gamma \sin 2\pi \frac{ky}{b}$$

where α $= \sum_1^H \sum_1^L F(h0l) \cos 2\pi \left(\frac{hx}{a} + \frac{lz_1}{c}\right)$

$$+ \sum_1^L \sum_{-L}^{-1} F(h0l) \cos 2\pi \left(\frac{hx}{a} + \frac{lz_1}{c}\right)$$

$$+ \sum_1^H F(h00) \cos 2\pi \frac{hx}{a} + \sum_1^L F(00l) \cos 2\pi \frac{lz_1}{c} + \frac{F(000)}{2}$$

$$= \sum_1^H \sum_1^L \left\{ \left[F(h0l) + F(h0\bar{l})\right] \cos 2\pi \frac{hx}{a} \cos 2\pi \frac{lz_1}{c} \right.$$

$$\left. + \left[-F(h0l) + F(h0\bar{l})\right] \sin 2\pi \frac{hx}{a} \sin 2\pi \frac{lz_1}{c} \right\}$$

$$+ \sum_1^H F(h00) \cos 2\pi \frac{hx}{a} + \sum_1^L F(00l) \cos 2\pi \frac{lz_1}{c} + \frac{F(000)}{2}$$

$$= p + \sum_1^H q \cos 2\pi \frac{hx}{a} - \sum_1^H r \sin 2\pi \frac{hx}{a}$$

where $p = \frac{F(000)}{2} + \sum_1^L F(00l) \cos 2\pi \frac{lz_1}{c}$

$$q = F(h00) + \sum_1^L \left[F(h0l) + F(h0\bar{l})\right] \cos 2\pi \frac{lz_1}{c}$$

$$r = \sum_1^L \left[F(h0l) - F(h0\bar{l})\right] \sin 2\pi \frac{lz_1}{c}$$

where β $= \sum_1^H \sum_1^L F(hkl) \cos 2\pi \left(\frac{hx}{a} + \frac{lz_1}{c}\right)$

$$+ \sum_1^H \sum_1^L F(h\bar{k}l) \cos 2\pi \left(\frac{hx}{a} + \frac{lz_1}{c}\right)$$

$$+ \sum_1^H \sum_{-L}^{-1} F(hkl) \cos 2\pi \left(\frac{hx}{a} + \frac{lz_1}{c}\right)$$

$$+ \sum_1^H \sum_{-L}^{-1} F(h\bar{k}l) \cos 2\pi \left(\frac{hx}{a} + \frac{lz_1}{c}\right)$$

$$+ (\text{over})$$

$$+ \sum_{1}^{L} F(0k\ell) \cos 2\pi \frac{\ell z_1}{c}$$
$$+ \sum_{1}^{L} F(0k\bar{\ell}) \cos 2\pi \frac{\ell z_1}{c}$$
$$+ \sum_{1}^{H} F(hk0) \cos 2\pi \frac{hx}{a}$$
$$+ \sum_{1}^{H} F(h\bar{k}0) \cos 2\pi \frac{hx}{a} + F(0k0).$$

$$= \sum_{1}^{H} \sum_{1}^{L} \left[F(hk\ell) + F(h\bar{k}\ell)\right] \left\{\cos 2\pi \frac{hx}{a} \cos 2\pi \frac{\ell z_1}{c} - \sin 2\pi \frac{hx}{a} \sin 2\pi \frac{\ell z_1}{c}\right\}$$
$$+ \sum_{1}^{H} \sum_{-L}^{-1} \left[F(hk\ell) + F(h\bar{k}\ell)\right] \left\{\cos 2\pi \frac{hx}{a} \cos 2\pi \frac{\ell z_1}{c} - \sin 2\pi \frac{hx}{a} \sin 2\pi \frac{\ell z_1}{c}\right\}$$
$$+ \sum_{1}^{L} \left[F(0k\ell) + F(0\bar{k}\ell)\right] \cos 2\pi \frac{\ell z_1}{c}$$
$$+ \sum_{1}^{H} \left[F(hk0) + F(h\bar{k}0)\right] \cos 2\pi \frac{hx}{a}$$
$$+ F(0k0)$$

$$= P + \sum_{1}^{H} Q \cos 2\pi \frac{hx}{a} - \sum_{1}^{H} R \sin 2\pi \frac{hx}{a}.$$

---

where $P = F(0k0) + \sum_{1}^{L} \left[F(0k\ell) + F(0\bar{k}\ell)\right] \cos 2\pi \frac{\ell z_1}{c}$

$$Q = \left[F(hk0) + F(h\bar{k}0)\right] + \sum_{1}^{L} \left[F(hk\ell) + F(h\bar{k}\ell) + F(hk\bar{\ell}) + F(h\bar{k}\bar{\ell})\right] \cos 2\pi \frac{\ell z_1}{c}$$

$$R = \sum_{1}^{L} \left[F(hk\ell) + F(h\bar{k}\ell) - F(hk\bar{\ell}) - F(h\bar{k}\bar{\ell})\right] \sin 2\pi \frac{\ell z_1}{c}$$

(over).

and where $\gamma = \sum_{1}^{H}\sum_{1}^{L}\left[F(hkl)-F(h\bar{k}l)\right]\left\{\sin 2\pi\frac{hx}{a}\cos 2\pi\frac{lz_1}{c} + \cos 2\pi\frac{hx}{a}\sin 2\pi\frac{lz_1}{c}\right\}$

$+\sum_{1}^{H}\sum_{-L}^{-1}\left[F(hkl)-F(h\bar{k}l)\right]\left\{\sin 2\pi\frac{hx}{a}\cos 2\pi\frac{lz_1}{c} + \cos 2\pi\frac{hx}{a}\sin 2\pi\frac{lz_1}{c}\right\}$

$+\sum_{1}^{L}\left[F(0kl)-F(0\bar{k}l)\right]\sin 2\pi\frac{lz_1}{c}$

$+\sum_{1}^{H}\left[F(hk0)-F(h\bar{k}0)\right]\sin 2\pi\frac{hx}{a}$

$= P + \sum_{1}^{H} Q\cos 2\pi\frac{hx}{a} + \sum_{1}^{H} R\sin 2\pi\frac{hx}{a}$

where $P = \sum_{1}^{L}\left[F(0kl)-F(0\bar{k}l)\right]\sin 2\pi\frac{lz_1}{c}$

$Q = \sum_{1}^{L}\left[F(hkl)-F(h\bar{k}l)-F(hk\bar{l})+F(h\bar{k}\bar{l})\right]\sin 2\pi\frac{lz_1}{c}$

$R = \left[F(hk0)-F(h\bar{k}0)\right]$

$+\sum_{1}^{L}\left[F(hkl)-F(h\bar{k}l)+F(hk\bar{l})-F(h\bar{k}\bar{l})\right]\cos 2\pi\frac{lz_1}{c}.$

There are thus three stages in the summation:

1 The terms are summed with respect to L and the figures occurring in the columns for a particular $z = z_1 = \frac{12}{30}c$ (say), are used.

2 & 3 These figures are then used in exactly the same way as that described by Lipson & Beevers (1936) for summation first with respect to H, and then finally, with respect to K.

To summarise:

$$V\rho(x,y,z_1) = \alpha + \sum_1^K \beta' \cos 2\pi k\frac{y}{b} - \sum_1^K \gamma \sin 2\pi k\frac{y}{b}$$

where $\alpha = \rho + \sum_1^H q \cos 2\pi h\frac{x}{a} - \sum_1^H s \sin 2\pi h\frac{x}{a}$.

$$\rho = \frac{F(000)}{2} + \sum_1^L F(00l)\cos 2\pi l\frac{z_1}{c}.$$

$$q = F(h00) + \sum_1^L \left[F(h0l)+F(h0\bar{l})\right]\cos 2\pi l\frac{z_1}{c}$$

$$s = \left[F(h0l)-F(h0\bar{l})\right]\sin 2\pi l\frac{z_1}{c}$$

where $\beta = P + \sum_1^H Q\cos 2\pi h\frac{x}{a} - \sum_1^H R\sin 2\pi h\frac{x}{a}$

$$P = F(0k0) + \sum_1^L \left[F(0kl)+F(0\bar{k}l)\right]\cos 2\pi l\frac{z_1}{c}$$

$$Q = \left[F(hk0)+F(h\bar{k}0)\right] + \sum_1^L \left[F(hkl)+F(h\bar{k}l)+F(hk\bar{l})+F(h\bar{k}\bar{l})\right]\cos 2\pi l\frac{z_1}{c}$$

$$R = \sum_1^L \left[F(hkl)+F(h\bar{k}l)-F(hk\bar{l})-F(h\bar{k}\bar{l})\right]\sin 2\pi l\frac{z_1}{c}$$

and where $\gamma = \mathcal{P} + \sum_1^H \mathcal{Q}\cos 2\pi h\frac{x}{a} + \sum_1^H \mathcal{R}\sin 2\pi h\frac{x}{a}$.

$$\mathcal{P} = \sum_1^L \left[F(0kl)-F(0\bar{k}l)\right]\sin 2\pi l\frac{z_1}{c}$$

$$\mathcal{Q} = \sum_1^L \left[F(hkl)-F(h\bar{k}l)-F(hk\bar{l})+F(h\bar{k}\bar{l})\right]\sin 2\pi l\frac{z_1}{c}$$

$$\mathcal{R} = \left[F(hk0)-F(h\bar{k}0)\right] + \sum_1^L \left[F(hkl)-F(h\bar{k}l)+F(hk\bar{l})-F(h\bar{k}\bar{l})\right]\cos 2\pi l\frac{z_1}{c}$$

Note: These equations may, of course be further simplified depending on the symmetry of the crystal.

Summations were made over enough sections to give the coordinates of all the atoms in the molecule without any ambiguity. Fig. 17 shows several sections, passing through two of the four molecules in the unit cell, projected along the c axis onto the ab plane. Fig. 18 gives the relevant parts of several sections passing through one molecule of para-chloriodoxy benzene, from which Fig. 17 was compiled.

It can be seen that the peaks due to the oxygen atoms are well resolved from the near by iodine peak. The benzene ring is not quite so clear.

Diagrams showing the structure projected onto the ab, bc, and ac planes are given in figs. 19, 20, and 21 respectively.

ESTIMATION OF PARAMETERS.

The coordinates of the iodine and chlorine atoms could be obtained with considerable accuracy from the three-dimensional Fourier sections shown in fig. 18, and these agreed very well with the coordinates obtained from the Fourier projections on the planes (010) and (001), shown in figs. 15, and 16.

The elongation of the iodine peak in the direction of the a axis is simply due to the shape of the equivalent optical aperture obtained by plotting the spectra on a reciprocal lattice net.

The coordinates of the atoms expressed as fractions of the corresponding lattice translations are given in Table 7.

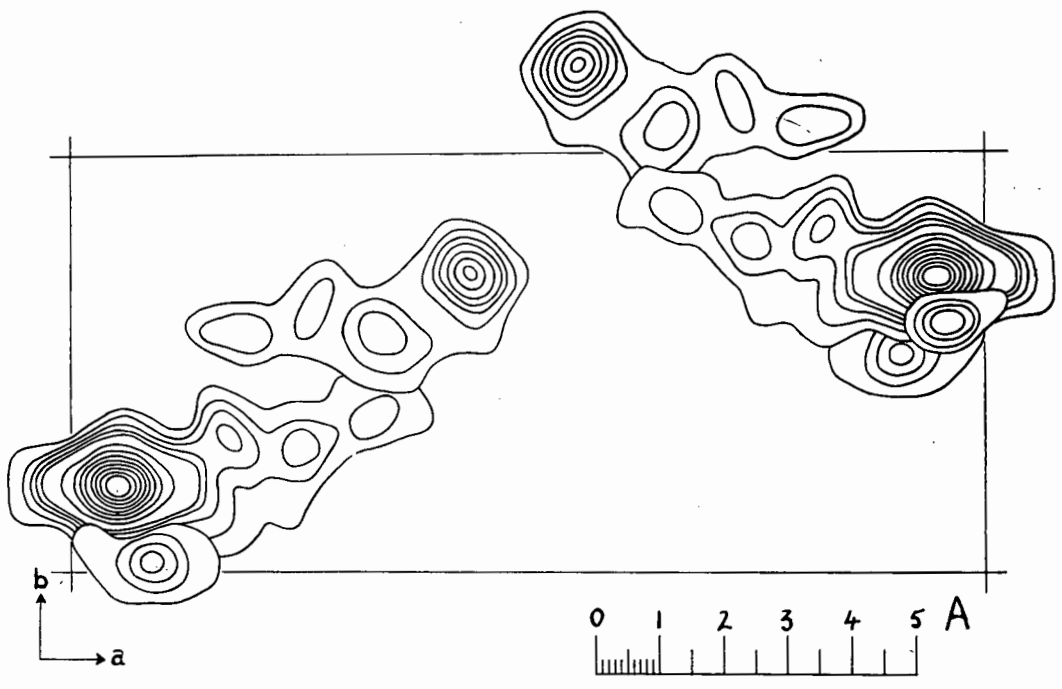

FIGURE 17. A projection along the c axis on to the ab plane of several 3-dimensional Fourier sections passing through two of the four molecules in the unit cell. Contours are drawn at arbitrary levels; 200, 400, 600, etc. For the iodine atom, contours above 1,000 are drawn at intervals of 1,000.

FIGURE 18. Parts of the three-dimensional Fourier sections parallel to the ab plane passing through one of the four molecules in the unit cell.

The sections are at intervals of c/30.

The contours in green are drawn at intervals of 200, while those in black are at intervals of 1,000.

The scale is 3 cms = 1A.

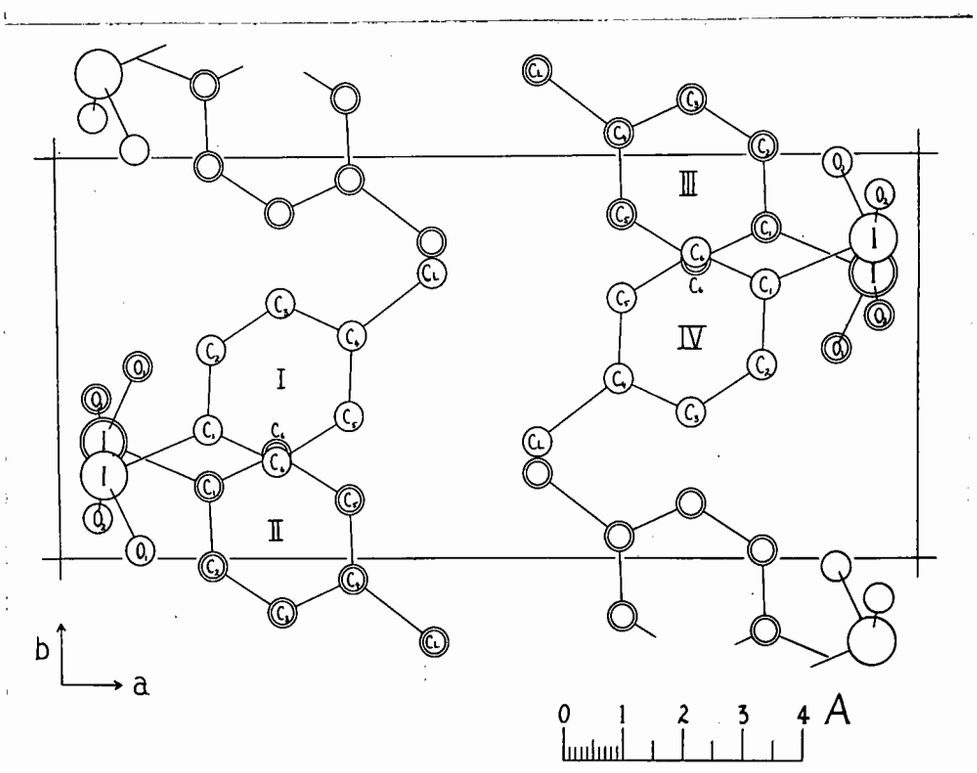

FIGURE 19. A projection of the structure in the c direction on to the ab plane. The molecules with double circles are c/2 above or below those with single circles.

$\frac{16}{30}$ c

$\frac{15}{30}$ c

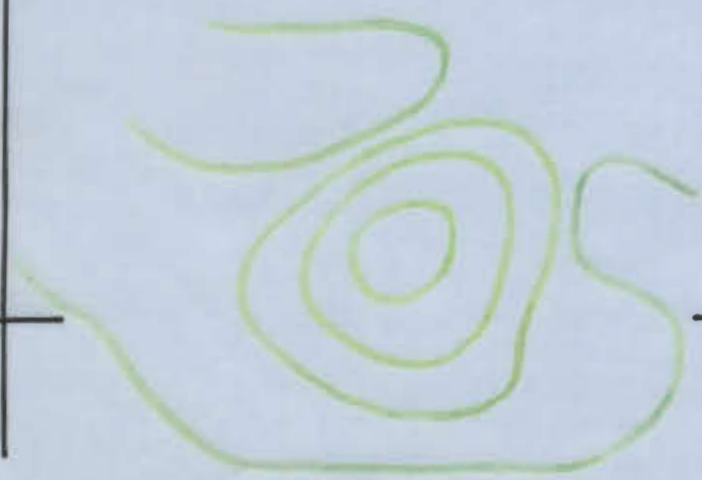

$\frac{14}{30}$ C

$\frac{13}{30}$ c

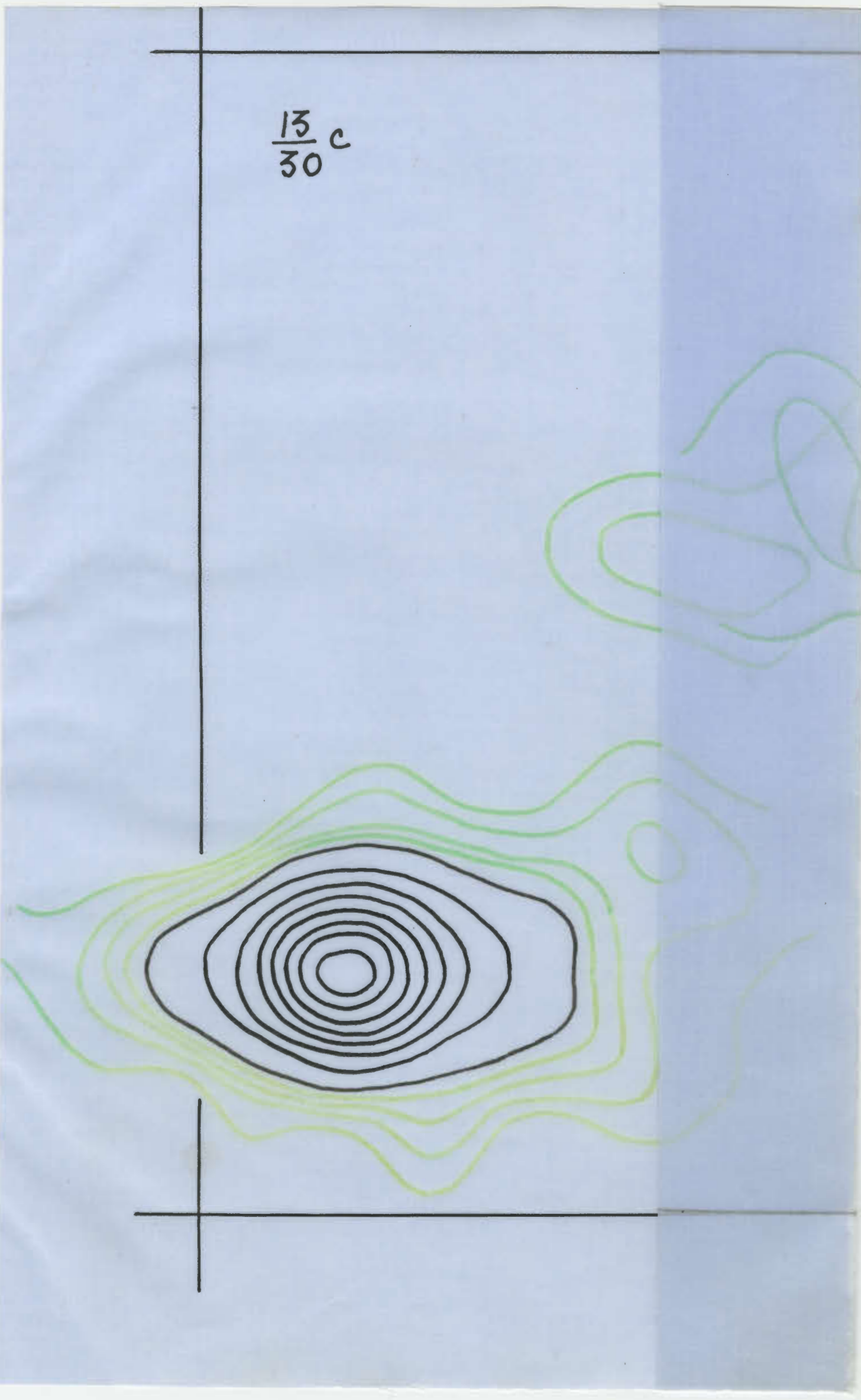

$\frac{12}{30}$ c

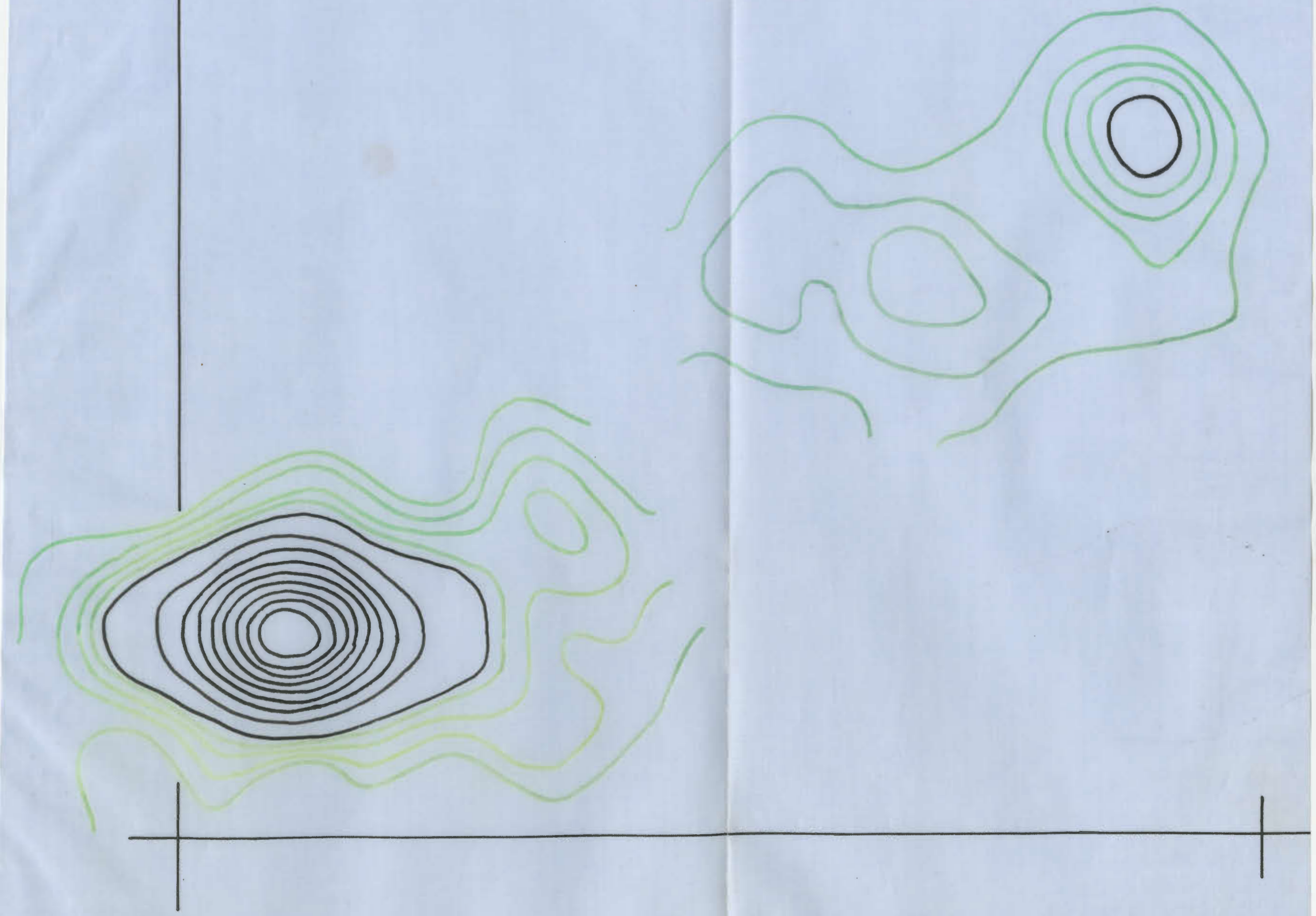

$\frac{11}{30}$ C

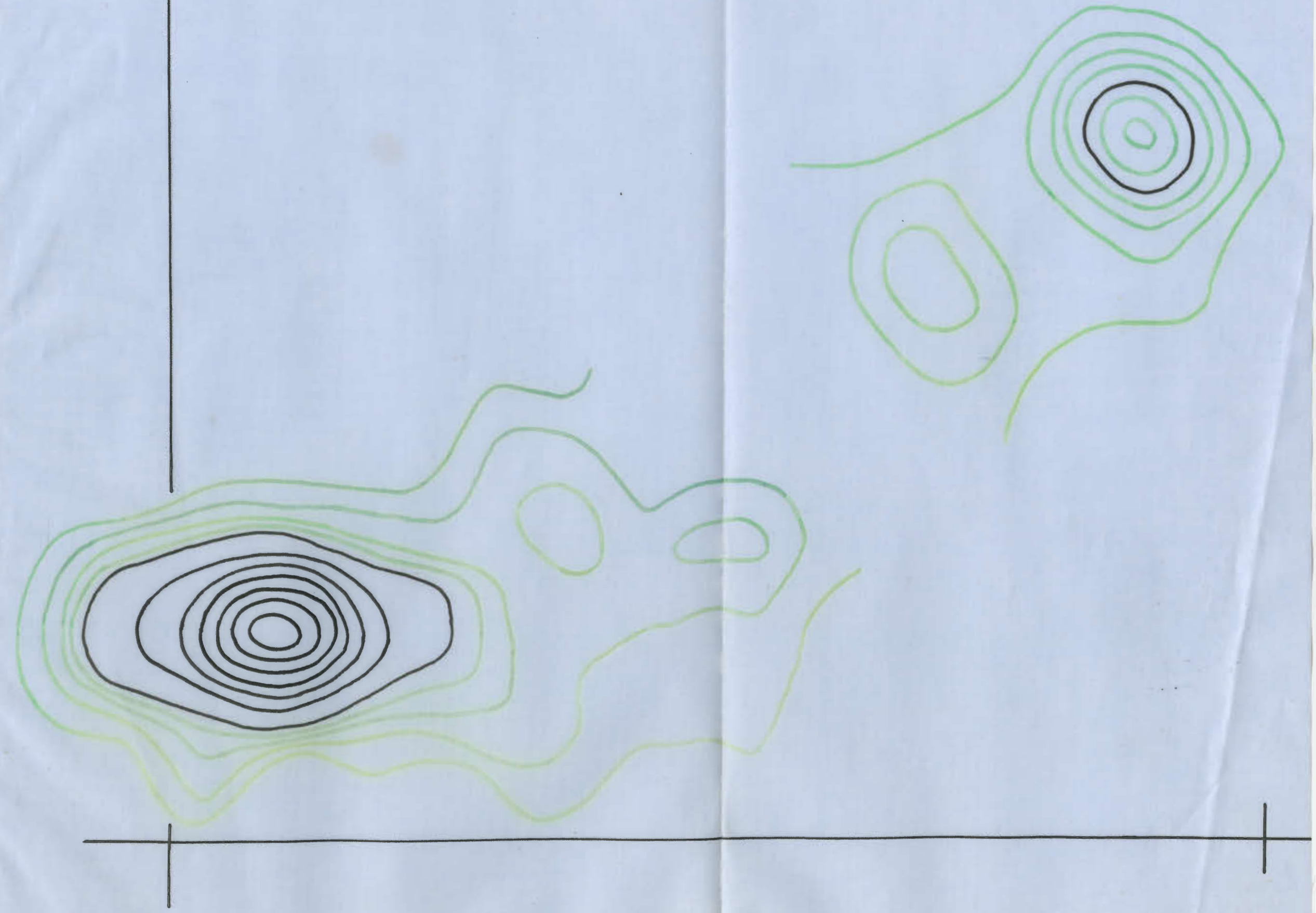

$\frac{10}{30}$ c

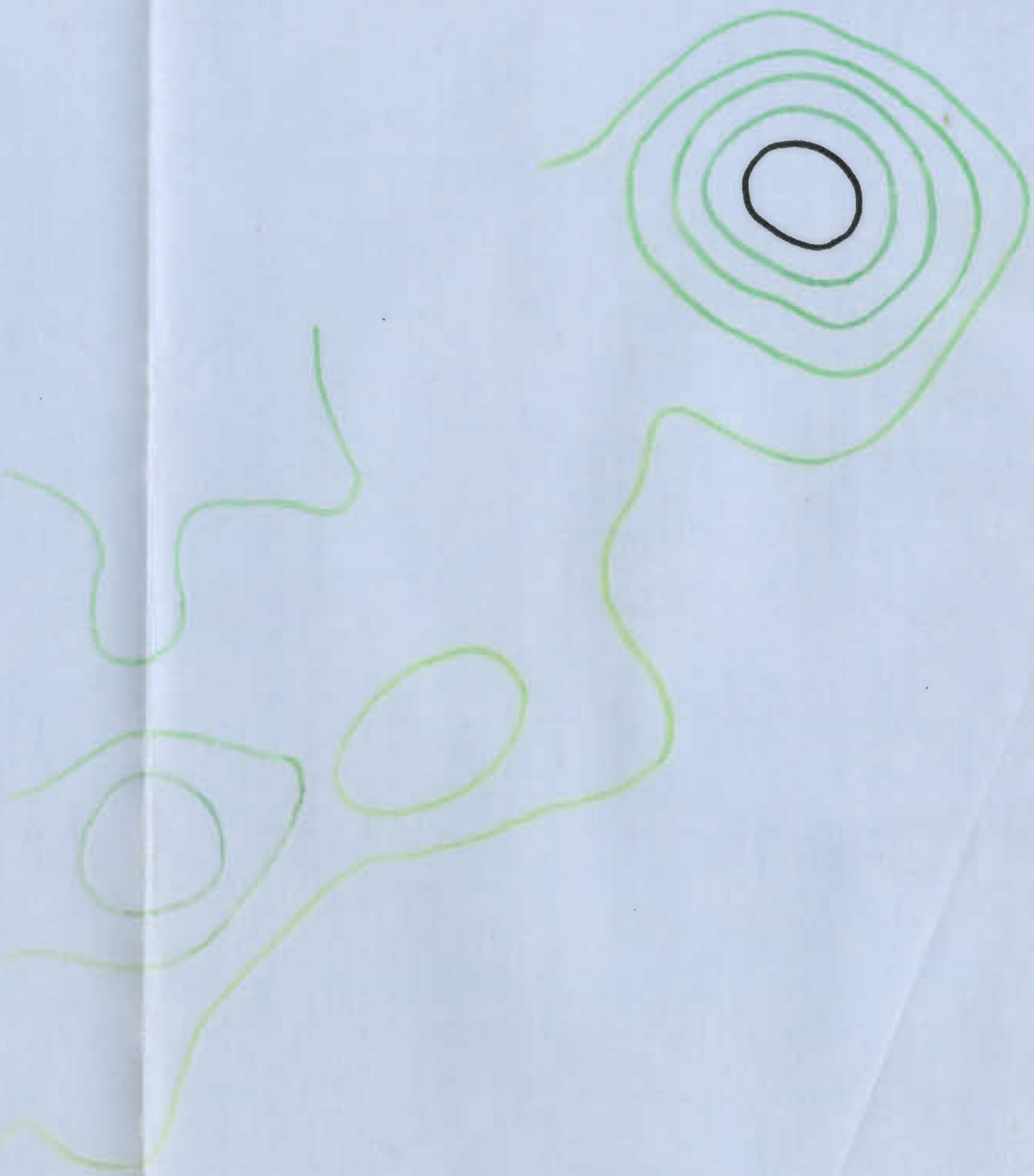

$\frac{9}{30}$ c

$\frac{8}{30}$ c

$\frac{7}{30}$ c

$\frac{6}{30}c$

$\frac{5}{30}$ c

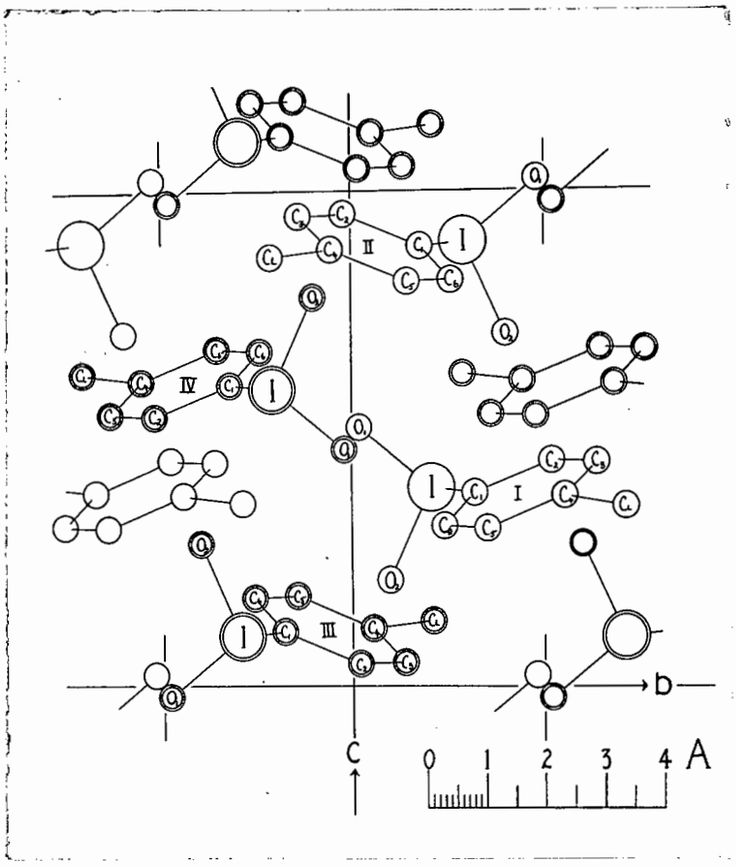

FIGURE 20. A projection of the structure in the a direction on to the bc plane. The molecules with double circles are appreximately a/2 above or below those with single circles.

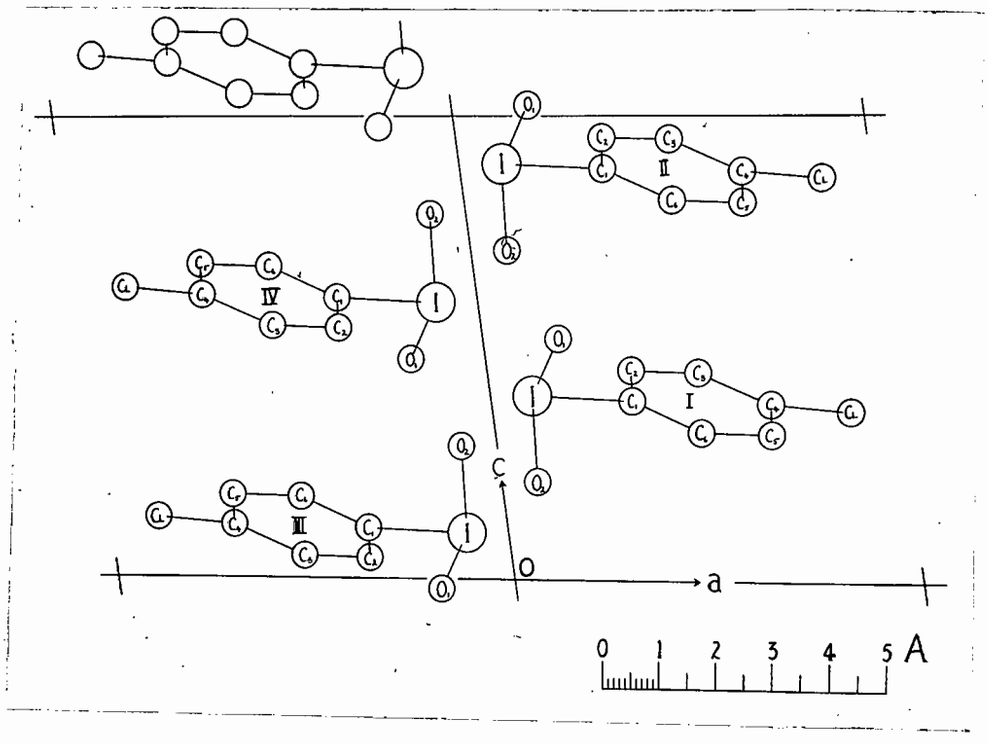

FIGURE 21. A projection of the structure in the b direction on to the ac plane.

TABLE 7. THE COORDINATES OF THE ATOMS EXPRESSED AS FRACTIONS OF THE CORRESPONDING LATTICE TRANSLATIONS.

	x/a	y/b	z/c
I	0.052	0.208	0.400
Cl	0.439	0.710	0.368
O_1	0.092	0.023	0.520
O_2	0.042	0.098	0.213
C_1	0.174	0.322	0.388
C_2	0.178	0.522	0.455
C_3	0.260	0.637	0.451
C_4	0.337	0.552	0.383
C_5	0.333	0.352	0.316
C_6	0.251	0.237	0.320

DESCRIPTION OF THE MOLECULE.

The size and shape of the molecule is given in fig. 22. It can be seen that the plane containing the iodoxy group is very nearly perpendicular to the plane of the benzene ring which in turn approximately bisects the angle $O\hat{I}O$.

The I-O distances 1.60A and 1.65A (±.05A) in para-chlor iodoxy benzene are rather shorter than those obtained in other compounds containing iodine and oxygen, which suggests the existence of double bonding between the iodine and oxygen atoms.

Table 8 compares the dimensions of the iodoxy group in para-chlor-iodoxy benzene with the dimensions found in iodine-oxygen groups in potassium fluoriodate (KIO_2F_2) and iodic acid (HIO_3) by Rogers and Helmholtz (1940, 1941), and ammonium paraperiodate ($(NH_4)_2H_3IO_6$) by Helmholtz (1937).

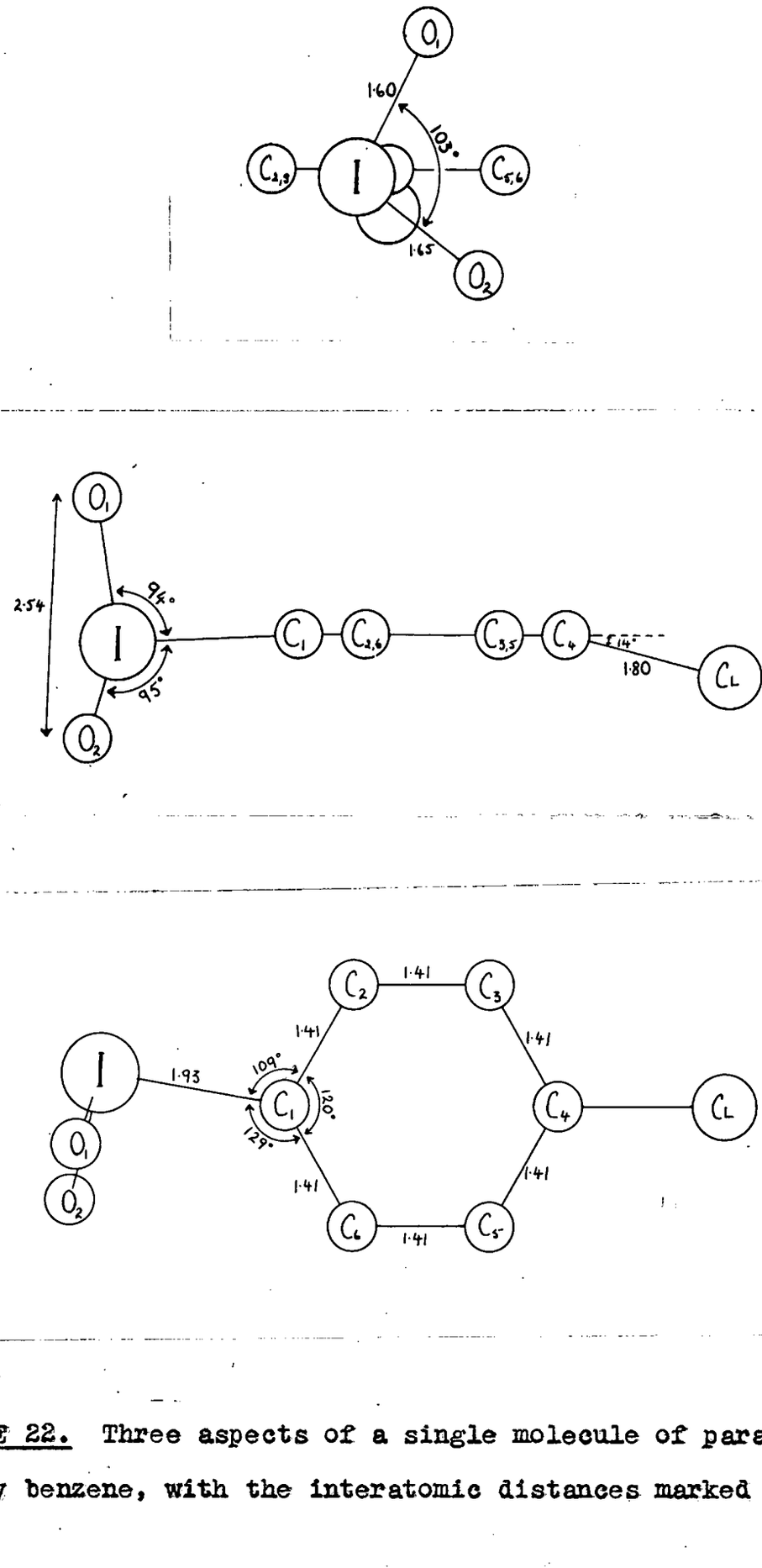

FIGURE 22. Three aspects of a single molecule of para-chloriodoxy benzene, with the interatomic distances marked in A.U.

TABLE 8. INTERATOMIC DISTANCES IN COMPOUNDS CONTAINING BOTH IODINE AND OXYGEN. (in A.U.)

	I-O in the same molecule	closest I to O between different molecules	closest O to O between different molecules	$O\hat{I}O$
para-chlor-iodoxy benzene	1.60 1.65	2.72 2.87	2.62	103°
iodic acid	1.80 1.81 1.89	2.45 2.70 2.95	2.76 2.78	96° 98° 101°
potassium fluoriodate	1.92 1.93	2.82 2.88	–	100°
ammonium paraperiodate	1.93	–	2.60	approx 90°

THE PACKING OF THE MOLECULES IN THE CRYSTAL.

There are 4 molecules in the unit cell which are derived from ~~one another~~ a single molecule by the operation of the glide plane and the two-fold screw axis. Figs. 19, 20, and 21 are labelled so that atoms derived from one another by the operation of a symmetry element are denoted by the same letter.

The iodoxy groups of the molecules approach one another very closely. The I to I distance between molecules I & IV and II & III is 3.60A whereas the usual I to I distance between different molecules is greater than 4.0A. An I to I distance of 3.79A between different molecules has been observed in iodic acid, and this short distance was attributed to the effect of unshared electrons in the molecules.

The I to O_1 distance between molecules I & IV and II & III is 2.72A and the I to O_2 distance between molecules I & II and IV & III is 2.87A, which distances are very much smaller than the sum of the iodine and oxygen ionic radii, namely 3.3A, but are comparable with the I to O distances observed between

different molecules in iodic acid and potassium fluoriodate. (see Table 8).

All the O to O distances are greater than 3.0A except the distance from O_1 to O_1 of molecules I & IV and II & III which is 2.62A. This is considerably shorter than the usual O to O distance between different molecules in organic compounds which is about 3.0A and slightly shorter than the normal O to O distance between molecules on inorganic compounds which is 2.7A. It is, however, comparable to the O to O distance observed in ammonium paraperiodate, 2.60A; which is attributed to hydrogen bonding. This theory is quite inapplicable in the case of para-chloriodoxy benzene. The O to O distances of 2.76A and 2.78A between different molecules in iodic acid have also been attributed to hydrogen bonding.

It can be seen that the I and O_1 of molecule I and the I and O_1 of molecule II form a very closely knit planar group with the bonds from I to O_2 very nearly perpendicular to this plane. Since the plane (001) is a cleavage plane in the crystal the strongest binding forces between different molecules are evidently in the plane formed by the I and O_1 atoms about a centre of symmetry.

All other distances in the crystal are large. The closest approach of CH groups in neighbouring benzene rings is 3.9A and the closest approach between neighbouring Cl atoms is 3.75A.

The interatomic distances described above are shown in fig. 23 .

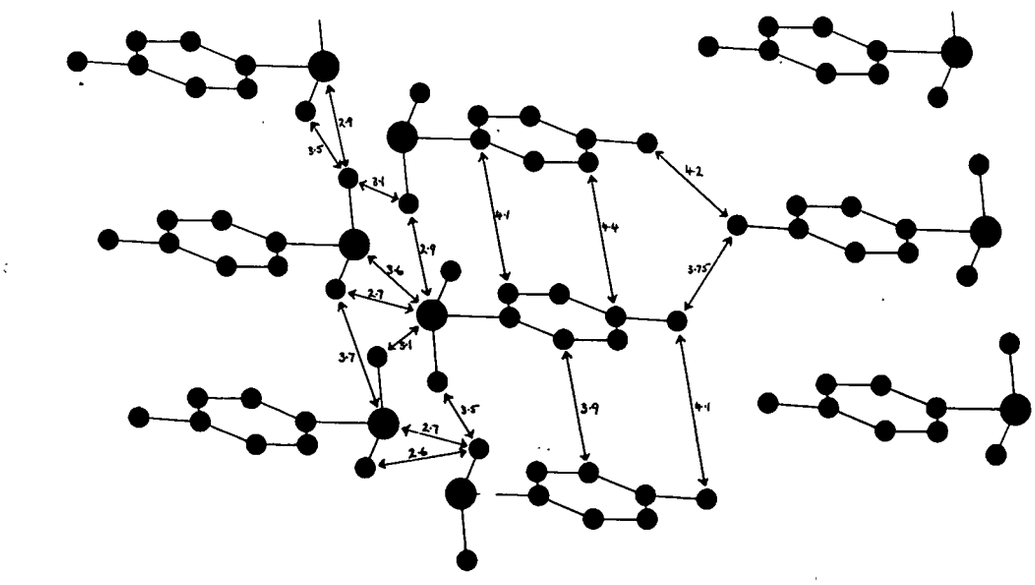

FIGURE 23. A projection of the structure on to the ac plane showing various interatomic distances marked in A.U.

DISCUSSION OF THE STRUCTURE.

The very close approach of iodoxy groups to one another, and the large distances between neighbouring benzene rings and chlorine atoms indicates that the main binding forces in the crystal occur between adjacent iodoxy groups. The fact that the crystal para-methyl-iodoxy benzene is identical with the crystal para-chlor-iodoxy benzene with regard to its space group, unit cell, and intensities of spectra shows that the replacement of the chlorine atom in the para-chlor-iodoxy benzene molecule with a methyl group has no effect on the packing together of the molecules which must therefore be determined mainly by the iodoxy groups.

In iodic acid and ammonium paraperiodate, close approaches of neighbouring oxygen atoms were attributed to hydrogen bonding. This theory is obviously untenable in the case of para-chlor-iodoxy benzene although the interatomic distances concerned are comparable with those observed in iodic acid and ammonium paraperiodate. (see Table 8)

The close approach of iodoxy groups to one another may be bound up with the "lone pair" of electrons attached to each iodine atom forming an attractive force between these groups other than the ordinary van der Waals' attraction between molecules. That there is some unusual attraction between neighbouring iodoxy groups cannot be disputed, but the nature of this force is a matter of conjecture.

THE CRYSTAL STRUCTURE OF

BENZENE IODO-DICHLORIDE.

PREPARATION AND DESCRIPTION OF THE CRYSTALS.

The benzene iodo-dichloride used in the experiments was prepared by passing pure, dry chlorine into a solution of iodobenzene in carbon tetrachloride. Yellow crystals of benzene iodo-dichloride separated out from the solution. Good crystals with brilliant reflecting faces were subsequently grown by the slow cooling of a solution in carbon tetrachloride. The crystals decompose fairly rapidly on exposure to the air and ultra-violet light so fresh crystals were grown for each set of photographs taken.

Benzene iodo-dichloride forms bright yellow, needle-shaped crystals belonging to the monoclinic system, with the elongation of the needles in the direction of the b axis. Faces giving goniometer reflections develop about the [010] zone, the common ones being (100), (001), and (101). The end faces (011) and $(01\bar{1})$ have been observed on some crystals.

The plane (001) is a cleavage plane of the crystal.

THE UNIT CELL AND SPACE GROUP.

Oscillation photographs were taken with CuK_α radiation and the dimensions of the unit cell are thus

$$a = 15.6\text{Å}$$

$$b = 5.44\text{Å}$$

$$c = 19.6\text{Å}$$

$$\beta = 90^\circ 30'$$

General reflections hkl occur only with $h+l = 2n$ showing that the unit cell is centred on the b face. Reflections $hk0$ occur with $h = 2n$, and $0kl$ with $l = 2n$. Reflections $h0l$ occur only with $h = 2n$ and $l = 2n$, and reflections $0k0$ only with $k = 2n$. Thus the space group is either $B_{2_1/a}$ or $B_{2_1/c}$ both of which are the same.

The space group has 8 equivalent points.

The density of the crystal , by the method of flotation is approximately 2.2 grms/c.c. which corresponds to 8 molecules of $C_6H_5ICl_2$ in a unit cell having the dimensions given above. Nothing in the structure is therefore fixed by symmetry.

The crystal can be referred to a primitive unit cell having the following dimensions

$$a = 15.6\text{Å}$$

$$b = 5.44\text{Å}$$

$$c = 12.3\text{Å}$$

$$\beta = 128^\circ 30'$$

The corresponding space group is $P2_1/a$.

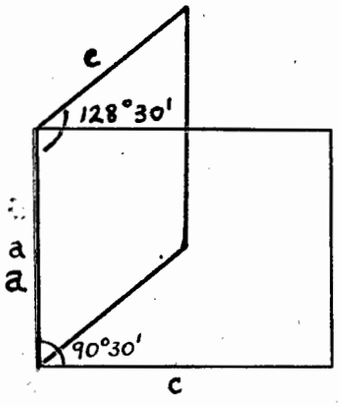

The axes referred to in this work are those with the monoclinic angle, $\beta = 90^\circ 30'$, since it was found more convenient to refer to these rather than to the primitive unit cell.

RELATIVE INTENSITY MEASUREMENTS.

All the observations were photographic, and were made on the normal-beam Weissenberg camera with CuK_α radiation filtered through nickel foil. The intensities of the spectra $h0\underline{l}$ and $0k\underline{l}$ were measured by comparing them visually with a calibrated scale of spots of different exposures.

The optimum thickness (t) of the crystal benzene iodo-

dichloride for CuK_α radiation was calculated from the linear absorption coefficient μ,

where $t = \frac{2}{\mu} = \frac{2}{377} = .0053$ cms.

Except for photographs with the crystal rotating about the b axis it is impossible to use crystals of such a cross-section. All the photographs were taken with crystals about .25 mm. thick and no corrections were made for absorption.

If MoK_α radiation is used, the optimum thickness for the crystal benzene iodo-dichloride is .043 cms. A series of photographs of crystals with approximately .25mm. cross-section have been taken with MoK_α radiation and these intensities measured on a microphotometer. No Fourier projections have yet been made using these more accurate determinations of intensity and so they are not included here.

STRUCTURE FACTOR CALCULATIONS.

The coordinates of a point in a general position for the space group $B2_1/a$ are

(x,y,z), $(x+\frac{1}{2}, y, z+\frac{1}{2})$, $(x+\frac{1}{2}, \frac{1}{2}-y, z)$, $(x, \frac{1}{2}-y, z+\frac{1}{2})$
$(\frac{1}{2}-x, y+\frac{1}{2}, \bar{z})$, $(\bar{x}, y+\frac{1}{2}, \frac{1}{2}-z)$, $(\bar{x}, \bar{y}, \bar{z})$, $(\frac{1}{2}-x, \bar{y}, \frac{1}{2}-z)$

The general structure factor F(hkl) is given by

$$F(hkl) = \sum_s f_s (A_s + iB_s)$$

The structure factors used in this work are F(h0l) and F(0kl).

For F(h0l) $\begin{cases} A = 8\cos 2\pi(hx+lz) \\ B = 0 \end{cases}$

For F(0kl) when k = 2n $\begin{cases} A = 8\cos 2\pi ky \cos 2\pi lz \\ B = 0 \end{cases}$

when k = 2n+1 $\begin{cases} A = -8\sin 2\pi ky \sin 2\pi lz \\ B = 0 \end{cases}$

TABLE 9. A COMPARISON OF F(observed) AND F(calculated) (FOR THE I AND C1ATOMS ONLY).

Spectrum	F(obs)	F(calc)	Spectrum	F(obs)	F(calc)
		8			8
200	25	-45	402	30	20
400	28	-19	404	18	20
600	41	41	406	18	16
800	35	-23	408	14	-17
14,00	13	-15	40,10	42	-54
			40,12	18	-35
020	26	-20			
040	9	- 9	$40\bar{2}$	51	-70
060	21	29	$40\bar{4}$	47	-46
			$40\bar{6}$	9	1
002	29	40	$40\bar{8}$	18	16
004	34	-12	$40,\bar{10}$	36	23
006	17	-19	$40,\bar{14}$	24	-33
008	29	-22	$40,\bar{16}$	22	-40
00,10	7	4			
00,12	41	46	602	5	7
00,14	19	38	604	9	-13
			606	37	-37
012	56	-27	608	30	-28
014	54	-47	60,10	9	20
016	23	-11	60,12	14	37
018	33	34			
01,10	34	29	$60\bar{2}$	53	49
01,12	5	8	$60\bar{6}$	49	-34
			$60\bar{8}$	22	-21
024	30	22	$60,\bar{12}$	19	19
026	37	32	$60,\bar{14}$	32	42
028	37	26			
02,10	8	6	802	28	-17
			806	27	27
032	5	11	808	36	52
			80,10	10	23
044	10	12			
048	13	9	$80\bar{2}$	11	2
			$80\bar{4}$	55	49
052	14	7	$80\bar{6}$	51	44
054	14	11	$80\bar{8}$	22	8
058	10	-20	$80,\bar{12}$	14	-20
05,10	9	-13			
			10,02	17	16
062	8	12	10,04	34	30
			10,08	14	-30
202	36	-51	10,0,10	10	-34
204	34	- 14			
206	11	7	$10,0\bar{2}$	30	-28
208	38	36	$10,0\bar{4}$	55	-45
20,10	40	38	$10,0\bar{8}$	19	22
20,14	14	-32	$10,0,\bar{10}$	14	18
			$10,0,\bar{16}$	12	-36
$20\bar{2}$	25	25			
$20\bar{4}$	42	48	12,04	20	-31
$20\bar{6}$	3	20	12,06	29	-44
$20,\bar{10}$	34	-29			
$20,\bar{12}$	46	-45	$12,0\bar{2}$	25	22
			$12,0\bar{6}$	29	-29
			$12,0\bar{8}$	30	-39

TABLE 9. (continued)

Spectrum	F(obs)	F(calc)/8
14,02	8	-23
14,0$\bar{6}$	30	40
14,0$\bar{8}$	10	22
16,02	14	31
16,04	12	32

TABLE 10. THE COORDINATES OF THE ATOMS EXPRESSED AS FRACTIONS OF THE CORRESPONDING LATTICE TRANSLATIONS.

	x	y	z
I	0.174	0.325	0.077
Cl_1	0.131	0	-0.003
Cl_2	0.218	0.650	0.156
C_1	0.056	0.325	0.116
C_2	0.038	0.276	0.172
C_3	-0.044	0.276	0.200
C_4	-0.110	0.326	0.170
C_5	-0.090	0.374	0.113
C_6	-0.008	0.374	0.086

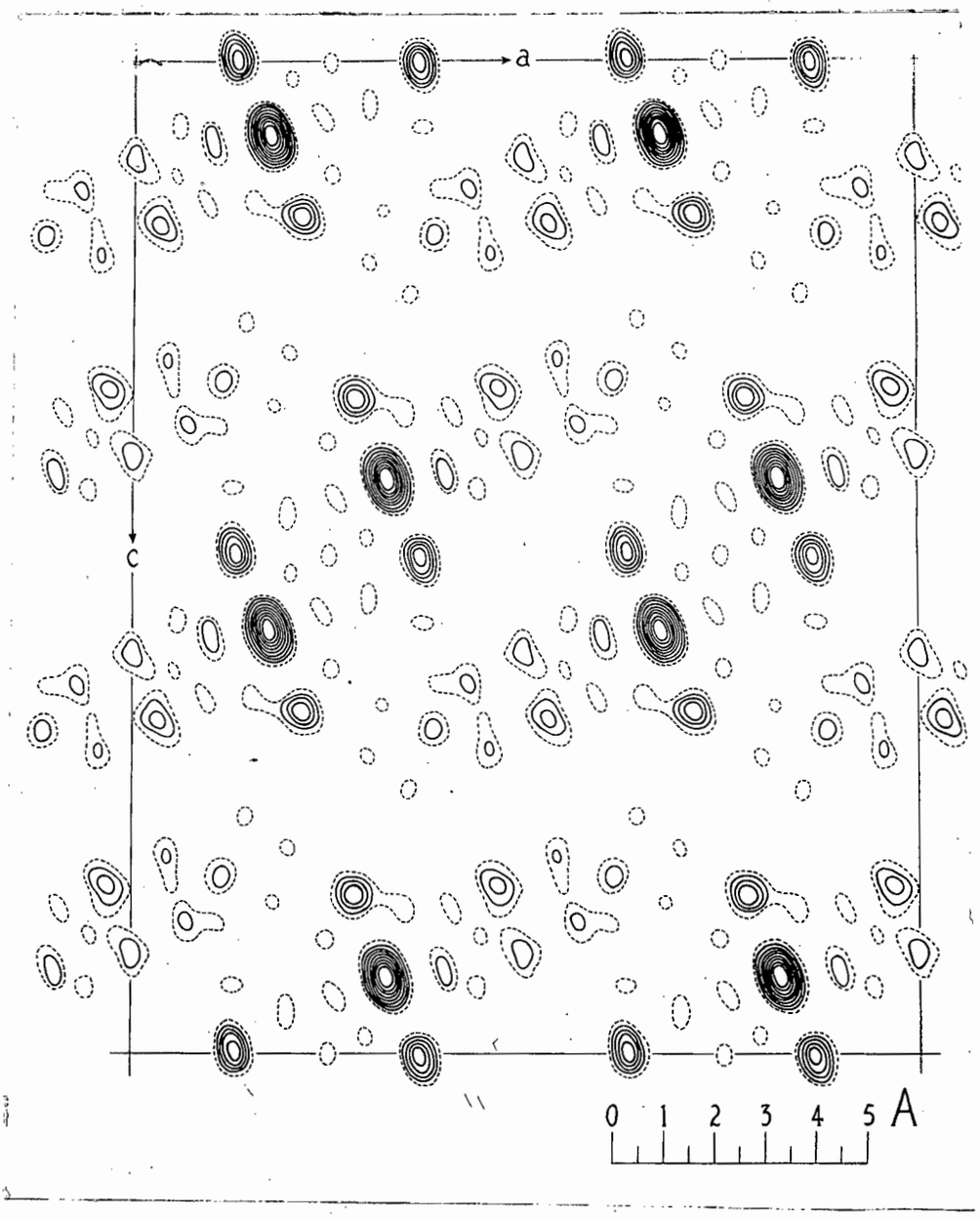

FIGURE 24. Fourier projection of the structure in the b direction on to the ac plane. The contours for the iodine atoms are drawn at intervals which are twice those between contours elsewhere.

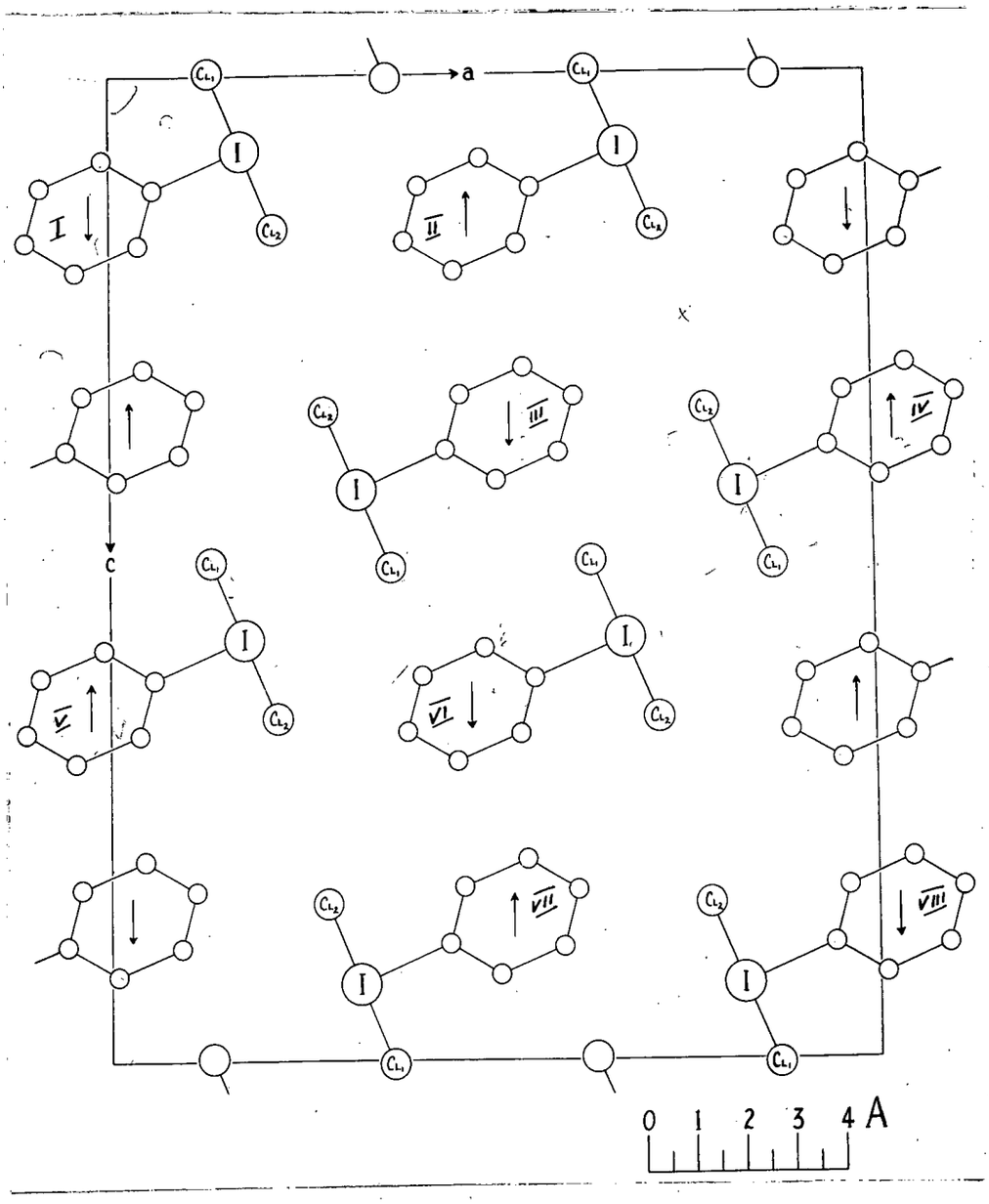

FIGURE 25. A projection of the structure in the b direction on to the ac plane. The arrows in the benzene rings denote tilts downwards.

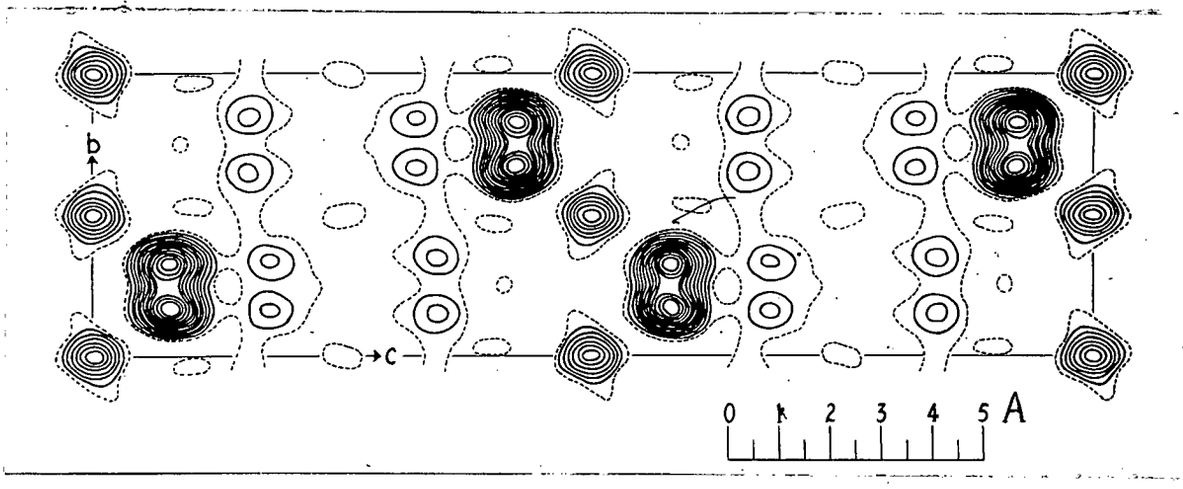

FIGURE 26. Fourier projection of the structure in the a direction on to the bc plane. All the contours are drawn at equal intervals.

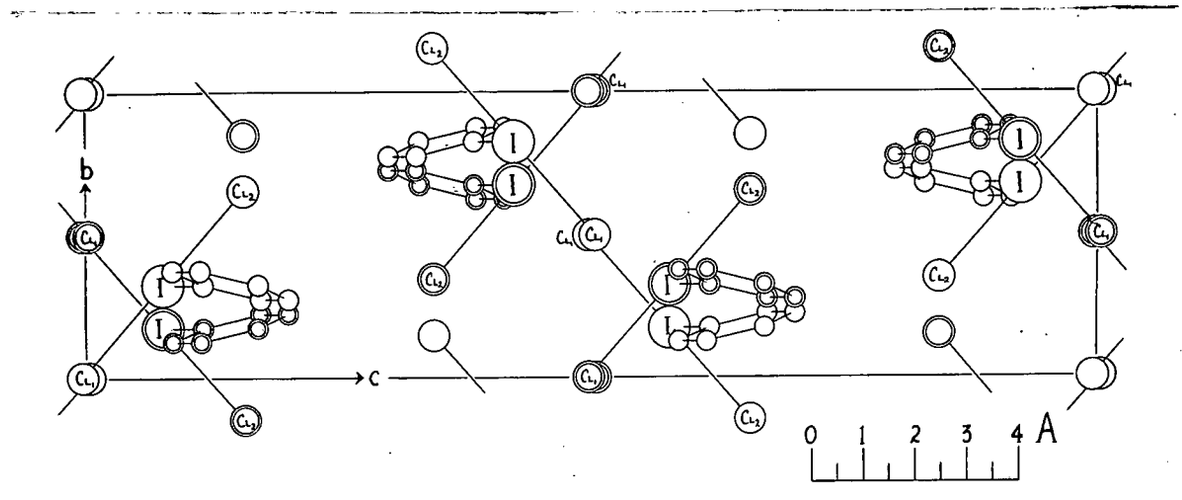

FIGURE 27. A projection of the structure in the a direction on to the bc plane. The molecules with double circles are a/2 above or below those with single circles.

THE FOURIER SYNTHESES.

The crystal has a centre of symmetry so the density $\sigma(x,z)$ of the projection of the structure at the point (x,z) on the ac plane is given by

$$\sigma(x,z) = \frac{1}{A(ac)} \sum_{-\infty}^{+\infty}_{h} \sum_{\ell} \pm |F(h0\ell)| \cos 2\pi \left(\frac{hx}{a} + \frac{\ell z}{c}\right)$$

where A(ac) is the area of the side ac of the unit cell.

The density of the projection of the structure at the point (y,z) on the bc plane is given by

$$\sigma(y,z) = \frac{1}{A(bc)} \sum_{-\infty}^{+\infty}_{k} \sum_{\ell} \pm |F(0k\ell)| \cos 2\pi \left(\frac{ky}{b} + \frac{\ell z}{c}\right)$$

The observed values of |F| are used as the coefficients in the series, the sign appropriate to any given coefficient being determined from the provisional structure. The projections were made using the method of Lipson and Beevers (1936).

The positions of the chlorine atoms showed up very clearly in the preliminary projections on the ac and bc planes. The position of the iodine atom had changed only very slightly from its assumed position. Structure factors were re-calculated using the improved position of the I atom and the coordinates assigned to the Cl atoms from the preliminary projections.

Second projections on the ac and bc planes were carried out and these are shown in figs. 24 and 26, together with the key diagrams figs 25 and 27.

There is a considerable amount of false detail in the projection on the ac plane, most of which is due to diffraction rings around the iodine atom. These rings occur in the positions calculated from the equivalent optical aperture, plotted in reciprocal space, put into the appropriate Bessel functions for the solution of diffraction effects. (see Appendix III). The elongation of the peaks of the iodine and chlorine atoms is accounted for by the shape of the equivalent optical aperture plotted in reciprocal space.

A projection on the ac plane was carried out using the signs used in the second projection but applying an artificial temperature factor of the form $e^{-B\frac{\sin^2\theta}{\lambda^2}}$, (B = 4), to the observed F values in order to eliminate the diffraction rings. (see Parker and Whitehouse (1932)). It was found that the diffraction rings disappeared and that the centres of the peaks belonging to the Cl atoms had moved about .1Å , making the I-Cl distance greater by nearly .1Å. (The positions of the 1st maximum of the diffraction rings is such that it would have this effect.)

The agreement between F(observed) and F(calculated) (for the second projection) is shown in Table 9 .

The interatomic distances quoted in the discussion of the structure are those calculated from the coordinates obtained from the second projection.

Table 10 gives the coordinates of the atoms expressed as fractions of the corresponding lattice translations.

DISCUSSION OF THE STRUCTURE.

It is evident from the projections on the ac and bc planes that the ICl_2 group is linear. The I-Cl distance is 2.45Å. This can be compared with the ICl_2 anion in tetramethylammonium dichloro-iodide ($N(CH_3)_4ICl_2$) by Mooney (1939) where the ICl_2 anion is linear with an I-Cl distance of 2.34Å.

The I-C_1 distance is 1.98Å and the benzene ring has been assumed to be a regular hexagon of side 1.41Å. The angles $C_1\hat{I}Cl_1$ and $C_1\hat{I}Cl_2$ are right angles.

It is worth pointing out that the ICl_2 group appears to have the same configuration, whether it is acting as an electrovalent group $N(CH_3)_4^+ ICl_2^-$ or as a single covalent group $C_6H_5-ICl_2$.

From the projections it seems probable that the plane

of the benzene ring is approximately perpendicular to the line $Cl_1 ICl_2$.

The closest approaches between different molecules occurs between the iodo-dichloride groups obtained from one another by means of the screw axis. (i.e. molecules III & V, IV & VI, and I & VII.)

These close approaches are from I to Cl_1, 3.47A, and from Cl_1 to Cl_1, 3.33A. Both these distances are somewhat shorter than the sums of the respective ionic radii. All other intermolecular distances between iodo-dichloride groups are greater than 4.0A. As the coordinates of the carbon atoms are rather uncertain no intermolecular distances, involving the carbon atoms, have been calculated.

THE TRIGONAL BIPYRAMID.

The valencies of trivalent iodine have been assumed to be directed towards the corners of a trigonal bipyramid, with the two "lone pairs" of electrons situated at the apexes. (Sidgwick and Powell, 1940).

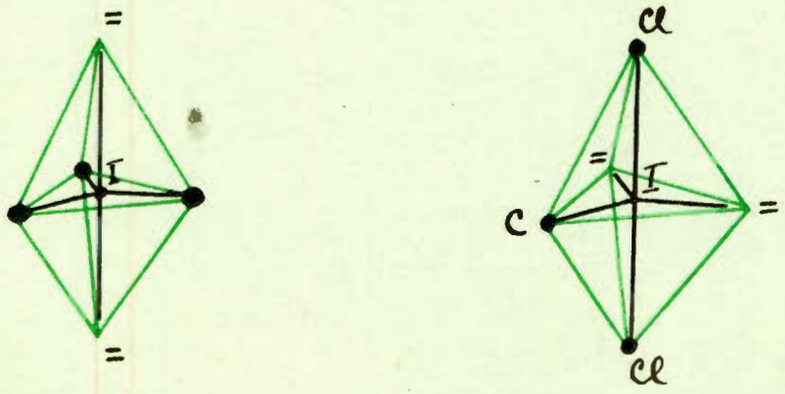

In order to fit a linear ICl group into the above scheme, the chlorine atoms would have to lie at the apexes and the "lone pairs" of electrons at the corners of the trigonal bipyramid.

Mooney (1935, 1938, 1939) has found that the tri-halogen groups in ammonium tri-iodide (NH_4I_3), ammonium bromo-chloro-iodide (NH_4BrICl) and tetramethylammonium dichloro-iodide ($N(CH_3)_4ICl_2$) are all linear. Following the present argument they could be represented thus:

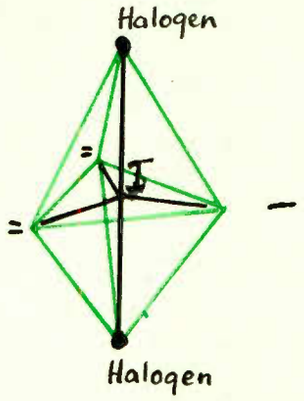

This scheme is also in keeping with the structure of potassium fluoriodate (KIO_2F_2) by Rogers and Helmholtz where the flouriodate ion can be represented diagrammatically thus:

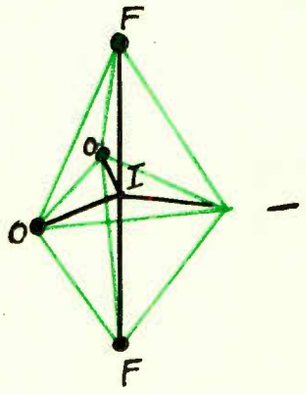

$O\hat{I}O = 100°$

although the iodine atom in this case is, however, 6-valent not trivalent.

THE SPATIAL VALENCIES OF IODINE.

The crystals para-chlor-iodoxy benzene and benzene iodo-dichloride were examined in order to determine, if possible, the valency directions of polyvalent iodine.

It has already been shown that the iodo-dichloride group in benzene iodo-dichloride can be fitted into the configuration of a trigonal bipyramid.

It is impossible, however, to fit the directions of the valency bonds in the iodoxy group in para-chlor-iodoxy benzene into any regular figure. Rogers and Helmholtz (1941) in their crystal structure of iodic acid (HIO_3) state that the bonds from the iodine atom to the oxygen atoms appear to be in the form of a distorted octahedron. (The angles of a regular octahedron are all 90°, whereas the angles found in iodic acid are about 100°). This "distortion" is rather more than can be accounted for by experimental error. The $\hat{OIO}$ angle in para-chlor-iodoxy benzene is 103°.

The theory that the valency bonds of the iodine atom are directed towards the corners of a regular octahedron is unsatisfactory, although it seems impossible to suggest an theory which would be satisfactory.

APPENDIX I.

X-RAY APPARATUS.

Two Machlett X-ray tubes emitting CuK_α radiation were used throughout this work and were supplied by the circuit shown diagrammatically in fig. 28. They are rated to operate at 50 K.V.P. and 15 mA but were generally operated at about 35 K.V.P. and 12 mA. The CuK_α radiation was partly absorbed by a filter of Nickel foil. The presence of Nickel as an impurity in both anticathodes was shown by the appearance of extra spots on the films corresponding to the NiK_α wavelength, and it was therefore necessary to exercise care in indexing the spectra.

The rotation camera, made by Unicam Instruments, Cambridge has a diameter of 60.0 mm and was equipped with goniometer arcs and collimator and telescope system. In addition to the 5°, 10°, and 15° cams originally fitted to the camera, extra cams of 30° and 50° were constructed and adapted for use with the camera.

The normal beam Weissenberg camera, constructed by Mr. R.D. Linton in the workshop of the University Physics Department, was of undistorted scale, having a diameter of 57.3 mm. and a travel of 2°/mm. It was also equipped with goniometer arcs and a telescope system and gave a total rotation of 200°.

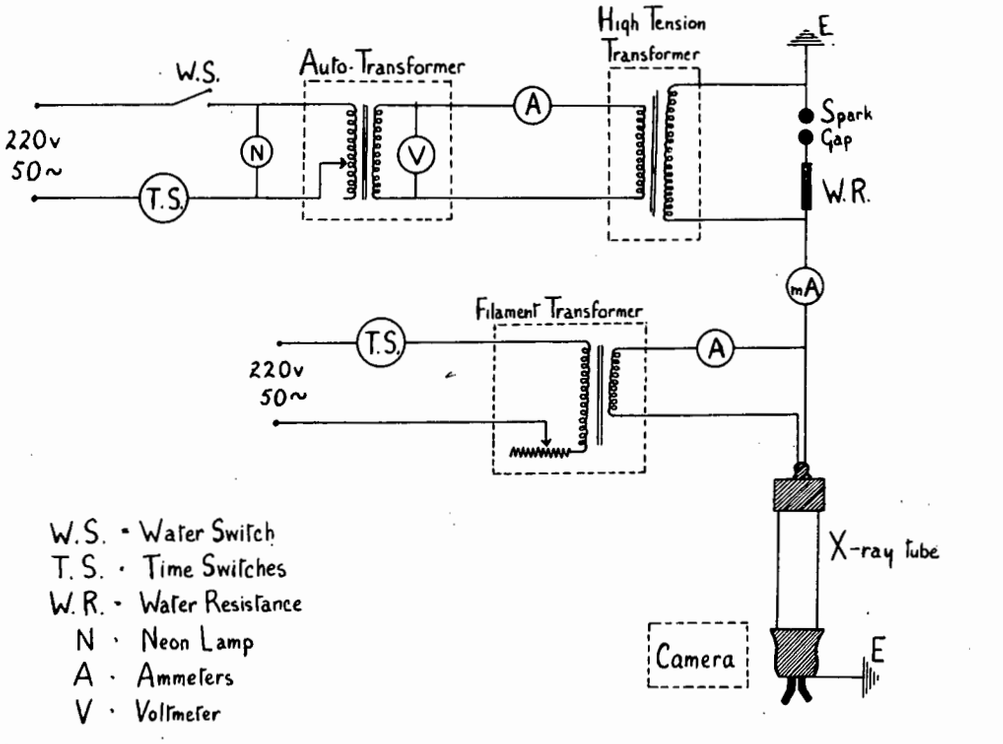

FIGURE 28. A diagrammatic representation of the X-ray apparatus used in the experiments.

APPENDIX 2.

THE STANDARD METHODS USED IN THE X-RAY ANALYSIS OF CRYSTALS.

Care was always exercised in choosing good crystal specimens. Suitable crystals were selected under a binocular microscope and generally had to be cut to approximately uniform cross-section about the desired axes. The crystals were mounted on the sharp point of a bakelite holder with a speck of either Canada Balsam or Secotine. The setting of the crystals was done using reflections from faces about the zone axes; when no faces were available however, the setting was adjusted by trial and error from the slope of the layer lines on the photographs.

The unit cells of the crystals and the indices of the spectra $\underline{hk}\underline{l}$ were determined using the standard reciprocal lattice methods developed by Ewald (1921) and applied by Bernal (1926) to graphical indexing.

The reciprocal lattice point $\underline{hk}\underline{l}$ can be referred to the cylindrical coordinates $\eta\, \xi\, \omega$ where η is the distance parallel to the rotation axis, ξ is the distance perpendicular to the rotation axis, and ω is the angular coordinate. The unit cells and general indices $\underline{hk}\underline{l}$ may be determined by measurement of the $\eta\xi$ coordinates of the spectra on rotation photographs using a Bernal chart. The reciprocal lattice points having those $\eta\, \xi$ coordinates may then be determined graphically. The indices of particular spectra of the type $\underline{h}00$, $\underline{h}0\underline{l}$, etc., are most easily determined by the measurement of the $\xi\, \omega$ coordinates on Weissenberg photographs using the $\xi\, \omega$ scales described by Buerger, and employing a similar graphical method.

When it was not possible to determine the monoclinic angle β from goniometer measurements, zero-layer line Weissenberg photographs were taken with a crystal rotating

about the b axis, and the angular separation of the h00 and 00l spectra measured.

APPENDIX 3.

THE FORMATION OF DIFFRACTION RINGS.

In general, the projections of point-like atoms made by using a limited number of spectra are not points, but are surrounded by diffraction rings.

This treatment of the formation of diffraction rings is substantially that given in Chapter 7 of "The Crystalline State" volume 2, by R.W. James.

Suppose the crystal structure to be projected along the b axis of the crystal which is perpendicular to the ac plane of the crystal lattice, and is also perpendicular to the a^*c^* plane of the reciprocal lattice. The reciprocal lattice points corresponding to the spectra h0l lie in this plane. Suppose that in making the projection all spectra, whose reciprocal lattice points lie on the plane within a distance R^* from the origin, are included. If θ_0 is the greatest glancing angle for any spectrum used, then

$$2 \sin \theta_0 \leq \lambda R^*$$

If A is the area of the mesh ac of the crystal lattice, the area of the reciprocal lattice mesh is 1/A, and a number of spectra approximately equal to $\pi R^{*2} A$ will be used in making the projection. The points in the reciprocal lattice plane are spread uniformly, with a surface density of A points per unit area.

When A becomes large, it will be shown that the series

$$\sigma(x,z) = \frac{1}{A(ac)} \sum_{h=-\infty}^{+\infty} \sum_{l} F(hol) \cos 2\pi \left(\frac{hx}{a} + \frac{lz}{c} \right)$$

tends to an integral in the limit.

For a simple lattice, where the unit of structure is a single atom, if one of the lattice points is taken at the origin, the values of $\delta(\underline{h}\underline{l})$ are all zero, and the coefficients $F(\underline{h}0\underline{l})$ are all positive and are all equal to $F(0)$.

The series then becomes

$$\sigma(x,z) = \frac{F(0)}{A} \sum_{-\infty}^{+\infty}{}' \sum_{\ell} \cos 2\pi \left(\frac{hx}{a} + \frac{\ell z}{c}\right)$$

$$\text{or} \quad \sigma(\underset{\sim}{r}) = \frac{F(0)}{A} \sum_{-\infty}^{+\infty}{}' \sum_{\ell} \cos 2\pi \left(\underset{\sim}{r} \cdot \underset{\sim}{r}^*\right)$$

where $\underset{\sim}{r}$ is the vector to the point (x,z) in the plane of the projection and $\underset{\sim}{r}^*$ is the reciprocal lattice vector to the point (h,l). The scalar product $\underset{\sim}{r}.\underset{\sim}{r}^*$ can be written $\underline{r}\underline{r}^*\cos\phi$ where ϕ is the angle between the directions of $\underset{\sim}{r}$ and $\underset{\sim}{r}^*$.

If A is very large, the vector $\underset{\sim}{r}^*$ to a reciprocal lattice point can be considered to be continuously variable. The element of area ds at the point $(\underline{r}^*, \phi)$ contains $Ar^*dr^*d\phi$ points, and together with the corresponding element of area at $(-\underline{r}^*, \phi+\pi)$ contributes an amount

$$2\frac{F(0)}{A} A r^* \cos 2\pi \left(\underset{\sim}{r} \cdot \underset{\sim}{r}^*\right) dr^* d\phi \quad \text{to} \quad \sigma(r).$$

The series can then be written

$$\sigma(r) = 2F(0) \int_0^{R^*} \int_0^{\pi} r^* \cos\left(2\pi r r^* \cos\phi\right) dr^* d\phi$$

This integral is one that occurs in the theory of diffraction by circular apertures, and contains a Bessel function of unit order. If $J_0(t)$ and $J_1(t)$ are Bessel functions of zero and unit order respectively, then

$$\int_0^{\pi} \cos(t\cos\phi)\, d\phi = \pi J_0(t)$$

$$\text{and} \quad \int_0^{z} t J_0(t)\, dt = z J_1(z)$$

By substitution,

$$\sigma(r) = 2\pi F(0) \int_0^{R^*} r^* J_0(2\pi r r^*)\, dr^*$$

$$i.e.\ \sigma(s) = 2F(0)\pi R^{*2}\frac{J_1(2\pi R^* s)}{2\pi R^* s}$$

This equation gives the value of the density $\sigma(r)$ at a distance r from one of the lattice points. The factor $F(0)\pi R^{*2}$ can be neglected in determining the distribution of density which is determined by the factor $\frac{2J_1(m)}{m}$ where $m = 2\pi R^* r$.

This factor has a principal maximum, equal to unity, at $m = 0$, and subsidiary lateral maxima and minima. The zero values are given by the roots of the equation $J_1(m) = 0$ with the exception of $m = 0$. The first four roots, other than $m = 0$, occur at values of m equal to 3.832, 7.016, 10.173, and 13.323. Thus the density $\sigma(r)$ is zero when

$$s = \frac{3.832}{2\pi R^*},\ \frac{7.016}{2\pi R^*},\ etc.$$

If R^* is not the same in all directions, i.e. if the equivalent optical aperture, plotted in reciprocal-lattice space is in the form of an ellipse, which is the case for the projection on the ac plane of the crystal benzene iodo-dichloride; then the peak formed in the projection $\sigma(x,z)$ will also be in the form of an ellipse, but with its major axis perpendicular to the major axis of the ~~crystal~~ elliptical aperture.

With the spectra h0l in benzene iodo-dichloride, the major axis of the elliptical aperture is in the direction of the reciprocal lattice point $40\bar{2}$, i.e. in a direction making an angle of 20° to the a^* axis, and has a value of $R^* = 1.10$. The minor axis is at right angles to this with a value of $R^* = .78$. If these values are put into the roots of the equation $J_1(m) = 0$, then, in the direction of the line C-I (see figs. 24, 25) the density $\sigma(r)$, due to the diffraction rings from the iodine atom, is zero when

$$r = \frac{3.832}{2\pi \times 1.10},\ \frac{7.016}{2\pi \times 1.10},\ \frac{10.173}{2\pi \times 1.10},\ \text{and}\ \frac{13.323}{2\pi \times 1.10}.$$

i.e. s = .56, 1.02, 1.47, and 1.93 (A.U.) from the centre of the iodine atom; and in the direction of the line Cl_1 I Cl_2 the density $\sigma(r)$ of the diffraction rings due to the iodine atom is zero when

$$r = \frac{3.832}{2\pi \times .78}, \quad \frac{7.016}{2\pi \times .78}, \quad \frac{10.173}{2\pi \times .78}, \text{ and } \frac{13.323}{2\pi \times .78}$$

= .78, 1.43, 2.07, 2.71 (A.U.) from the centre of the iodine atom. Since the I-Cl distance in benzene iodo-dichloride is 2.45A it can be seen that the first maximum of the diffraction rings in this direction tends to displace the peaks due to the chlorine atoms towards the iodine atom. This is in agreement with the results obtained by applying an artificial temperature factor to the observed F(h0l) in order to eliminate the diffraction rings.

A C K N O W L E D G E M E N T S.

I particularly wish to thank Professor R.W. James for his constant personal interest and advice throughout the course of this work. I am further indebted to him for the use of unpublished data on the crystal meta-dinitrobenzene, and also for the use of his unpublished manuscript of "The Crystalline State" volume 2. I wish to thank Dr. W.S. Rapson for suggesting the problem of the valency directions of polyvalent iodine, and for preparing the crystals used in the experiments. I also wish to thank Dr. M. Lamchen for the interest he took in this work, and his suggestions on some of the chemical problems involved.

I am grateful to Mr. R.D. Linton for being ever ready to undertake the construction and repairing of apparatus.

BIBLIOGRAPHY.

Bamberger & Hill Ber. 33, 533, (1900).

Banerjee & Bhattacharjya Science & Culture, 4, 60, (1938).

Banerjee & Ganguly Ind. J. Phys. 14, 231, (1940).

Bernal Proc.Roy. Soc. A, 113, 118, (1926).

Booth Trans. Farad. Soc. 41, 434, (1945).

Ewald Z. Krist. A, 56, 148, (1921).

Gregory & Lassettre J. A. C. S. 69, 102, (1947).

Harker Jour. Chem. Phys. 4, 381, (1936).

Helmholtz J. A. C. S. 59, 2036, (1937).

Hendricks & Hibbert J. A. C. S. 53, 4280, (1931)

Hertel Z. Phys. Chem. B, 7, 188, (1930).

James & Brindley Phil. Mag. 12, 81, (1931).

James, King, & Horrocks Proc. Roy. Soc. A, 153, 225, (1935).

Lipson & Beevers Proc. Phys. Soc. 48, 772, (1936).

Lonsdale Proc.Phys.Soc. 52, 314, (1942).

Lonsdale & Orelkin Proc. Roy. Soc. A, 144, 630, (1934).

Mooney Z. Krist. 90, 143, (1935).

Mooney Z. Krist. 98, 324, (1938).

Mooney Z. Krist. 100, 519, (1939).

Parker & Whitehouse Phil. Mag. 14, 939, (1932).

Robertson Proc. Roy. Soc. A 50, 106, (1935).

Rogers & Helmholtz J. A. C. S. 62, 1537, (1940).

Rogers & Helmholtz J. A. C. S. 63, 278, (1941).

Saunder Proc. Roy. Soc. A. 188, 31, (1946).

Saunder, "The Crystal Structure and Constitution of some Molecular Complexes of 4:4'-dinitrodiphenyl", Thesis presented to the University of Cape Town (1947).

Sidgwick & Powell Proc. Roy. Soc. A. 26, 153, (1940).

Steinmetz Z. Krist. 54, 467, (1915).

van Niekerk Proc. Roy. Soc. A. 181, 314, (1943).

van Niekerk, "An X-ray Study of the Internal Structure of Certain Crystals, with Special Reference to 4:4'-dinitrodiphenyl", Thesis presented to the University of Cape Town (1941).

Willgerodt Ber. 26, 1948, (1893).

General References.

Bragg, W. H. & W. L., "The Crystalline State", vol. 1

James, R. W., The Crystalline State", vol. 2.

Buerger, M. J., "X-Ray Crystallography".

"Internationale Tabellen zur Bestimmung von Kristallstrukturen", vols. 1 & 2.

Lonsdale, K., "Structure Factor Tables".